Transcriptional, metabolic and epigenetic changes associated with *in utero* diesel exhaust particulate exposure

Jamie Michelle Goodson

A dissertation

submitted in partial fulfillment of the

requirements for the degree of

Doctor of Philosophy

University of Washington

2017

Reading Committee:

Michael T. Chin, Chair

Christine M. Disteche

Terrance J. Kavanagh

Program Authorized to Offer Degree:

Pathology

University of Washington

Abstract

Transcriptional, metabolic and epigenetic changes associated with *in utero* diesel exhaust particulate exposure

Jamie Michelle Goodson

Chair of the Supervisory Committee:

Associate Professor Michael T. Chin

Cardiology Division, Department of Medicine

In utero exposure to diesel exhaust air pollution has been associated with increased adult susceptibility to heart failure in mice but the mechanisms by which this exposure promotes susceptibility are poorly understood. To identify potential transcriptional effects that mediate this susceptibility, we have performed RNA-seq analysis on neonatal cardiomyocytes from mice exposed to diesel exhaust *in utero,* as well as on adult hearts that have undergone transverse aortic constriction. We have identified a neonatal cardiomyocyte dysregulation of 300 genes, including many involved in cardiac metabolism. In the adult hearts, we have identified three target genes, *Mir133a-2*, *Ptprf* and *Pamr1*, which demonstrate dysregulation after exposure and aortic constriction. These target genes in the heart are the first to be identified that likely play an important role in mediating adult sensitivity to heart failure.

We followed up on the identified neonatal transcriptional dysregulation by determining whether cardiomyocytes from mice exposed *in utero* to diesel exhaust have impaired metabolic activity. We observed that the neonatal cardiomyocytes exhibit reduced metabolic activity as measured by pyruvate/glutamate-fueled oxygen consumption. However, the adult mitochondria showed a conflicting increase in metabolic activity as measured by pyruvate/glutamate-fueled respiration, as well as an increased mitochondrial load as measured by the ratio of mitochondrial:genomic DNA.

We subsequently examined for DNA methylation modifications both in global regulatory regions and at these candidate loci in neonatal cardiomyocytes after *in utero* exposure to diesel exhaust and found hypomethylation both globally at CpG-rich regions and in the first exon of GM6307, the gene *miR133a-2* is intronically embedded in. We have shown a change in DNA methylation within cardiomyocytes as a result of *in utero* exposure to diesel exhaust. Taken together, we have demonstrated that *in utero* exposure to diesel exhaust alters the neonatal cardiomyocyte transcriptional and epigenetic landscapes, as well as the metabolic capability of these cells, and that when these mice undergo heart failure as adults, there are changes in gene expression related to both heart failure and the *in utero* exposure.

Table of Contents

List of Abbreviations

3-NT – 3-Nitrotyrosine

AMA – antimycin A

CHD – congenital heart defect

CRP – C-reactive protein

DE – diesel exhaust

DOHaD – developmental origins of health and disease

FA – filtered air

FCCP – Carbonyl cyanide-p-trifluoromethoxyphenylhydrazone

hmC – hydroxymethylcytosine

IUGR – intrauterine growth restriction

MBP – methyl-binding proteins

NCM – neonatal cardiomyocyte

mC – methylcytosine

mtDNA – mitochondrial DNA

RCR – respiratory control ratio

ROS – reactive oxygen species

Rot – rotenone

RRBS – reduced representation bisulfite sequencing

TAC – transverse aortic constriction

List of Figures

List of Tables

Acknowledgements

I am extremely grateful to my thesis advisor, Dr. Michael Chin, for his mentorship, encouragement, and endless optimism throughout my research. I would especially like to thank our collaborators at the Center for Exposures, Diseases, Genomics and Environment, Dr. Theo Bammler and James MacDonald for their expertise in the statistical analysis of our datasets. I would also like to thank Dr. Rong Tian and lab members for support with running the Seahorse metabolic experiments, as well as Dr. David Marcinek and lab members for assistance in running the Oxygraph metabolic experiments. I am grateful to my committee members Drs. Christine Disteche, Terrance Kavanagh, Robb MacLellan and Michael Rosenfeld. I would especially like to thank Drs. Michael Chin, Christine Disteche and Terrance Kavanagh for reading my dissertation. I am thankful everyday for the best cohort anybody could ask for, and the support of my friends and family, especially my mother, Cyndi. Finally, I am forever grateful to my wonderful husband, Michael, for all of his support and encouragement throughout this journey.

Chapter 1

Introduction

Air-pollution has been long studied for its impact on human health, including impacts on pulmonary disease [1-3], cerebrovascular diseases such as stroke [4, 5] and cardiovascular disease [6-8]. Air pollution consists of a gaseous component and a particulate matter component. Particulate matter is classified by size, ranging from coarse particulate matter that is less than 10 μm in diameter (PM_{10}), fine particulate matter ($PM_{2.5}$) and ultrafine particulate matter ($PM_{0.1}$). The PM composition is determined by its source, with many traffic-sourced PMs containing polycyclic aromatic hydrocarbons, oxidative metals such as copper and iron, and elemental carbon. The gaseous component of air pollution can include carbon monoxide and dioxide (CO and CO_2 respectively), nitrogen and sulfur oxides (NO_x and SO_x respectively), and ozone (O_3) [9]. These components have been studied both individually and in the broad context of air pollution for their contribution to pathological disorders. There is a great interest in understanding how *in utero* exposure can affect fetal and early life health as more studies are published demonstrating the harmful effects of maternal exposure. The Barker hypothesis, also known as the developmental origins of health and disease (DOHaD) hypothesis, proposes that conditions of fetal distress such as hypoxia or malnutrition have strong impacts on adult health [10, 11]. By further understanding how maternal exposure is affecting fetal growth

and health, we can better predict, prevent and treat health issues that might arise during pregnancy or early life.

In utero exposure to air pollution and placental effects

The placenta serves many important roles in fetal development, and understanding how maternal exposure can impact placental health is critical. A recent study in the Netherlands using a prospective pregnancy cohort, called the Generation R Study, analyzed markers of placental health and size. The researchers found that increased PM_{10} and NO_2 exposures were correlated with higher fetal expression of the gene sFlt-1, an anti-angiogenic tyrosine kinase, as measured in cord blood, and that increased exposure two months prior to delivery was associated with significantly decreased placental weight [12]. A study of placental weight in relation to maternal proximity to major roads found that not only was placental weight significantly lower when mothers lived within 200m of a major road, but the placental/birth weight ratio was significantly higher [13], which is a marker of decreased placental efficiency [14]. Animal studies have found that maternal exposure to diesel exhaust in rabbits had significantly decreased placental blood flow and placental efficiency [15], and that gestational exposure in mice results in significantly decreased placental weight [16, 17], as well as a significant placental upregulation of proinflammatory transcripts such as IL-2 and IL-5 [18].

One of the common hallmarks of exposure to air pollution is increased inflammation, either directly through immune cells such as increasing white blood

cell [19] and platelet count [20], or through increasing expression of immune mediators such as C-reactive protein (CRP) [20, 21] and IL-6 [22, 23]. Increased inflammation during pregnancy can lead to fetal complications like preterm birth [24, 25] and preeclampsia [26]. Investigations into maternal exposure to air pollution and inflammatory response have found that $PM_{2.5}$ and PM_{10} exposure during early pregnancy are associated with increased maternal CRP [27], and that increased exposure to PM_{10} or NO_2 throughout pregnancy is associated with elevated fetal CRP levels [28]. Our lab has used mouse models to show that exposure to diesel exhaust during gestation is associated with placental necrosis and hemorrhage, as well as a significant increase in infiltrating CD45+ cells, suggesting a white blood cell response to exposure [16]. Additionally, we observed a significant increase in placental 3-nitrotyrosine (3-NT), a marker of nitrative stress, and a finding that has been replicated in human studies using the Belgian ENVIR*ON*AGE birth cohort, linking increased exposure to $PM_{2.5}$ and increased levels of placental 3-NT [29].

Placental mitochondrial DNA (mtDNA) has been of recent interest for linking maternal exposure and fetal health. A publication by Janssen *et al* used the ENVIR*ON*AGE birth cohort to study the negative association between PM_{10} and placental mtDNA [30]. They found that for each 10 $\mu g/m^3$ increase in maternal PM_{10} exposure during the third trimester, there was a roughly 10% decrease in placental mtDNA. Additionally, substituting distance between maternal home and major roads for exposure level showed an increase of roughly 4% placental mtDNA for each doubling of the distance. In both PM_{10}

exposure and distance from major road, there was no observed difference in cord blood mtDNA. Similar associations between NO_2 exposure and placental mtDNA were observed.

A separate study looking at the association between maternal exposure to NO_2 and placental mtDNA combined the ENVIR*ON*AGE cohort and the INMA birth cohort from Spain [31]. Their repeat of analysis of the ENVIR*ON*AGE placental mtDNA found significantly decreased mtDNA for each 10 $\mu g/m^3$ of maternal NO_2 exposure during the second and third trimester, and the entire pregnancy. Using the INMA cohort, they observed a significant decrease in mtDNA during each trimester, as well as the entire pregnancy. Combining the two cohorts, they found a significant association between NO_2 exposure during the second and third trimester, as well as the entire pregnancy, and decreased placental mtDNA. Additionally, they analyzed the relation between the observed NO_2 exposures and birth weight. While the ENVIR*ON*AGE cohort showed no significant association between exposure and birth weight, the INMA showed a significant decrease in birth weight resulting from NO_2 exposure, roughly -66g for each 10 $\mu g/m^3$ increase in NO_2. Pooling both cohorts retained the significant association, with -47g for each 10 $\mu g/m^3$ NO_2 increase. Finally, they studied the association between placental mtDNA and birth weight, finding that increased placental mtDNA was associated with increased birth weight.

These results were followed up in the INMA cohort by analyzing infant growth in the first year, and it was found that increased exposure to NO_2 during the first trimester strongly and negatively correlates with infant height in the first 6

months and infant weight in the first year, and that the levels of placental mtDNA were positively associated with height at birth and 6 months [32]. These studies highlight a potential mechanism linking maternal exposure and altered fetal health, as a decreased capacity for placental energy generation could negatively impact fetal growth, which has significant impacts on early life development and health [33].

In utero exposure to air pollution and fetal and newborn effects

Maternal exposure to air pollution has been found to negatively impact preterm birth and birth weight [34-36], and this association is strongly impacted by location. These findings of maternal exposure linked to decreased newborn weight, are concerning as intrauterine growth restriction (IUGR) is a well-known factor in the development of cardiovascular disease in adulthood [11, 37, 38]. However, reports on this issue vary widely depending on location, methods of measurement and statistical stringency. One study using the INMA birth cohort in Spain looking at maternal exposure to NO_2 and benzene and preterm birth showed that exposure to NO_2 > 46.2 μg/m^3 and benzene levels > 2.7 μg/m^3 throughout the pregnancy significantly increased the risk of preterm births [39]. In contrast, a study of the PIAMA birth cohort in the Netherlands found no significant association between NO_2, $PM_{2.5}$, or soot exposure during pregnancy and birth weight [40]. However, exposure to NO_2 in the PIAMA study was much lower, with the participants not reaching exposure levels of even 40 μg/m^3 until the 95th percentile. A study in Norway found that increased maternal exposure to

NO_2 was associated with lower birth weight, especially when the exposure was >20 $\mu g/m^3$ [41]. Yet, while the association was significant when accounting for birth season, child's sex, and maternal age, height, education, marital status and smoking, the association was lost once either home location or maternal weight was included in the analysis. Still, a meta-analysis of study centers covering nine countries, and with a total samples size of over 3 million births, found that increased exposure to both $PM_{2.5}$ and PM_{10} are significantly associated with decreased newborn weight [42], signifying that exposure to air pollution has a measureable effect on newborn weight.

Maternal exposure to air pollution has also been linked to decreased fetal weight. A study of PM_{10} and NO_2 maternal exposure using the Generation R Study cohort found that both were negatively correlated with second trimester head circumference, and that NO_2 was negatively correlated with fetal femur length in the second and third trimester [43]. Similarly, a study in Sweden found that maternal exposure to various NO_x was negatively associated with fetal femur length and estimated weight in the second trimester, as well as newborn weight [44].

Finally, a small number of studies have been carried out looking at other newborn health effects. A study of newborn blood pressure found that maternal exposure to increased $PM_{2.5}$ and black carbon during the third trimester of pregnancy correlated to higher newborn blood pressure, while exposure to O_3 was negatively correlated [45]. A separate study found an association between NO_2 exposure in the third trimester and increased childhood blood pressure [46].

While significant, it is unclear how these findings would impact early life and adult health, though it has been shown that childhood blood pressure is maintained to adulthood [47].

In utero exposure to air pollution and early life and adult effects

Maternal exposure to air pollution negatively affects the newborn condition, which in turn has long reaching effects on early life, development and adult health. It is necessary to understand and characterize these early risk factors to better understand the impact of air pollution. For the purposes of this review, I will focus on early life and adult effects centering on cardiac conditions.

There has been growing interest in studies linking maternal exposure to air pollution and congenital heart defects (CHD). A study of congenital defects in England found that there was an association between maternal exposure to SO_2 and tetralogy of Fallot [48]. Similarly, a study in Texas found that there was a significant correlation between maternal exposure to CO and tetralogy of Fallot, as well as PM_{10} and increased risk of isolated atrial septal defects [49]. A recent cohort study in China found that increasing maternal exposure to $PM_{2.5}$ during early pregnancy was associated with increased risk of CHD [50].

While there have been few studies of adult cardiac health directly related to *in utero* exposure to air pollution, a study of college students at the University of Southern California found that increased prenatal exposure to $PM_{2.5}$ and PM_{10} are associated with increased carotid arterial stiffness, a predictor of future cardiovascular dysfunction, but not with changes in blood pressure, heart rate or

carotid artery intima-media thickness [51]. No correlation between any of these cardiac outcomes and prenatal NO_2 or O_3 exposure was identified. Interestingly, the researchers identified no effect of postnatal exposure to $PM_{2.5}$ or PM_{10} on carotid arterial stiffness, highlighting the importance of prenatal exposure.

Given the challenges of epidemiological studies linking gestational exposure and adult cardiovascular disease, animal studies have been helpful in exploring these links [16, 52-54]. Our studies in C57BL/6 mice have shown that gestational exposure to diesel exhaust (DE; average ~50 μg/m^3/hr, 6 hrs/day, 5 days/week) is sufficient to create increased adult susceptibility to heart failure after transverse aortic constriction, demonstrated by significantly increased left ventricular anterior wall thickness and decreased fractional shortening as compared to filtered air (FA) controls [16]. Similarly, a study in FVB mice found that *in utero* exposure to $PM_{2.5}$ (average ~70 μg/m^3/hr, 6 hrs/day, 7 days/week) was sufficient to produce baseline dysfunction, demonstrated by decreased fractional shortening and cardiomyocyte contractility, and that there was a significant decrease in protein expression of SERCA-2A and NCX suggesting possible defects in calcium handling [53]. While understanding the impacts of gestational exposure on human health is important, animal models are significantly easier to manipulate in order to test the many hypotheses generated by epidemiological studies. These studies, taken with evidence of the long-term impact of maternal exposure to air pollution on human health, signal the need to look further into the mechanisms behind maternal exposure and fetal impact.

Potential mechanisms for maternal exposure and cardiac reprogramming

Adult exposure is thought to affect cardiovascular health through three possible mechanisms: 1) inflammatory response in the lungs spilling to other sites, 2) autonomic nervous system imbalance through particle interaction with nerves in the lung, or 3) particles moving into the blood stream and interacting with distant cells [6]. It is unclear whether any of these mechanisms have any effect on maternal exposure and fetal outcomes, especially due to potential effects of exposure on the mother's health. Air pollution is known to have adverse effects on respiratory health, including asthma [55, 56], so it is possible that these effects could be mediated by compromised maternal respiration leading to fetal hypoxia [57].

As mentioned previously, many cases of air pollution exposure are linked to an increased inflammatory response. Given the findings that maternal exposure can impact adult cardiac health, it would be reasonable to assume that if this mechanism is mediated at least in part by activation of the immune system then alternative models of maternal inflammation should yield similar effects. The link between maternal inflammation, preterm birth and IUGR has been well established [24, 25, 58]. In the same vein, oxidative stress has been found to play an important role in the impairment of fetal growth [59]. The findings of decreased placental mitochondrial load [30, 31] could be caused by oxidative stress damaging mitochondria, as they are susceptible to oxidative damage [60]. Discoveries of increased placental 3-NT [16, 29], as well as evidence of increased oxidative damage in maternal blood as measured by mitochondrial 8-

OHdG [61], implicate a role for nitrative and oxidative stress in the development of fetal and newborn growth restriction.

A role for epigenetic alteration after exposure has been gaining traction. There has been evidence of alterations in epigenetic control via decreased LINE-1 methylation, indicative a depressed global methylation, due to air pollution exposure in adults [62, 63]. Interestingly, C57BL/CBA mice exposed to ambient air pollution showed increased DNA methylation in sperm [64], which could be a potential mechanism by which exposure in the adult can cause defects in the offspring. While the studies linking maternal exposure and fetal epigenetic alterations have been few, a number have shown an associated decrease in LINE-1 methylation following maternal exposure [46, 65, 66], suggesting another role for oxidative damage by way of inhibiting normal DNA methylation maintenance [67].

Despite numerous studies linking maternal exposure to air pollution and fetal outcomes, the mechanism(s) by which exposure negatively impacts fetal health are largely unknown. Available animal models of maternal exposure and fetal health facilitate mechanistic studies, as they allow for manipulations not possible in human studies. By understanding the underlying cardiovascular disruptions in the offspring exposed *in utero* to air pollution, we can begin to elucidate the mechanisms driving dysfunction, as well as identify potential avenues of treatment.

Chapter 2

In utero exposure to diesel exhaust particulates is associated with an altered cardiac transcriptional response to transverse aortic constriction and altered DNA methylation

2.1 INTRODUCTION

Exposure to particulate matter air pollution has been associated with respiratory [2, 3], cardiovascular [6, 68, 69] and cerebrovascular [4] disease. Exposure to fine particulate matter (particulates ≤ 2.5μm, or $PM_{2.5}$) has been linked to increased cardiovascular morbidity and mortality [6]. Early life exposure to $PM_{2.5}$ has been increasingly recognized for its impact on newborn health. Exposure to PM_{10} during pregnancy has been linked with decreased birth weight, reduced placental weight [43] and placental oxidative/nitrative stress [29], further suggesting particulate matter air pollution to contribute to placental insufficiency and IUGR. Placental insufficiency and IUGR has been implicated as an important determinant of adult cardiovascular health through the “fetal origins of adult disease” or “Barker Hypothesis” pathway [11]. These *in utero* PM exposures that induce placental insufficiency may predispose offspring to increased risk of disease, and indeed, exposure to $PM_{2.5}$ during the last trimester of pregnancy has been reported to be associated with increased newborn systolic blood pressure [45]. While prospective studies have not yet been carried out to determine whether these effects of maternal exposure affect the health of the offspring into adulthood, experimental studies using animal models raise the

concern that *in utero* exposure to air pollution may be a strong determinant of adult health.

We have previously shown that *in utero* and early life exposure to diesel exhaust (DE) air pollution increases adult susceptibility to heart failure in mice, where after transverse aortic constriction (TAC) surgery, we observed decreased fractional shortening and increased left ventricular hypertrophy when compared to filtered air (FA) exposed control animals [16, 52]. We have also reported that this increased adult susceptibility to heart failure is conferred with an *in utero* exposure only, highlighting the importance of the gestational window in mediating this long lasting effect. Although we have identified placental vascular oxidative stress and inflammation as possible physiological mechanisms, the molecular basis of increased heart failure susceptibility that persists from gestation to adulthood has not yet been elucidated.

One potential molecular mechanism to explain our observation of increased susceptibility to heart failure following *in utero* DE exposure involves epigenetic modification and altered transcription of key mediators. Air pollution has been shown to alter DNA methylation both globally and at specific target genes. Human workplace exposure to PM_{10} has been found to be associated with global hypomethylation at LINE-1 and Alu repetitive DNA elements in circulating leukocytes, as well as decreased methylation at the *iNOS* promoter [63]. A study of exposure to $PM_{2.5}$ showed a similar hypomethylation of DNA in peripheral blood leukocyte DNA [62]. Exposure to $PM_{2.5}$ during pregnancy has been associated with altered global DNA methylation profiles within placental

tissue, where increased $PM_{2.5}$ exposure was associated with lower global DNA methylation [70]. This observation supports the hypothesis that developing fetal tissues *in utero* may be subject to particulate matter-induced alterations in DNA methylation. Altered DNA methylation in the developing myocardium as a result of exposure could persist to adulthood and influence transcription of genes related to heart failure in our mouse model. To identify DE-responsive target genes that may be relevant to heart failure, we performed RNA-sequencing of adult heart mRNA after *in utero* exposure to either DE or FA followed by either TAC or sham surgery as adults, and have identified three potential target genes: *Mir133a-2*, *Ptprf* and *Pamr1.* To determine whether alterations in DNA-methylation may play a role in differential expression of these genes, we performed targeted bisulfite sequencing on the CpG islands and promoters associated with these genes. We discuss the associated changes in DNA methylation and the potential role of these genes in mediating the increased susceptibility to heart failure observed in this model.

2. 2 METHODS

Diesel exhaust exposure and mice

C57BL/6 male and female mice were purchased from The Jackson Laboratory (Bar Harbor, Maine, USA) and maintained as an inbred line. All mice were housed in specific pathogen free conditions (SPF) on a 12/12-light/dark cycle. Female and male mice between the ages of 12 to 14 weeks were

transferred to our Northlake Diesel Exposure Facility located near the University of Washington (UW) and housed under SPF conditions in Allentown caging systems (Allentown, NJ, USA) as previously described [16, 52, 71-74]. All animal experiments were approved by the UW Institutional Animal Care and Use Committee. The protocol number is 4134-01 and the date of approval was 13 June 2016. Diesel exhaust was generated from a single cylinder Yanmar diesel engine (Model YDG5500EV-6EI) operating on 82% load. A detailed analysis of DE particulate components in this system has been previously reported [72]. DE exposures were conducted for 6 hours per day (9 am – 3 pm) five days a week (Monday – Friday) and DE concentrations were regulated to ≈ 300 μg/m^3 of $PM_{2.5}$. A 300 μg/m^3 concentration of $PM_{2.5}$ six hours/day, five days/week equates to a time weighted hourly average of 53 μg/m^3. Exposure characteristics detailing gas, particle-bound polycyclic aromatic hydrocarbons (PAH), and particle diameter were recently measured and reported [52, 74].

Female mice were paired with male mice for timed mating in FA. After observation of a vaginal plug, pregnant mice were put into FA or DE with exposures beginning at E0.5 and lasting until E17.5. Neonates were used for neonatal cardiomyocyte preparation (described below) or saved for adult surgery. Offspring were raised in FA until 11 weeks, at which time they underwent baseline echocardiography and transverse aortic constriction at 12 weeks using a 27-gauge needle. Serial echocardiographic measurement, gravimetry and histology for these mice have been previously published [16]. Hearts from these mice were harvested at 15 weeks, rapidly frozen in liquid nitrogen and stored at -

80^{o}C prior to RNA isolation. The *in utero* exposure and sample collection scheme is displayed in Figure 2.1.

RNA isolation, sequencing and bioinformatics analysis

RNA was isolated from fresh frozen hearts of three mice per group using the Qiagen (Germantown; MD, USA) miRNeasy kit according to the manufacturer's protocol. RNA-Seq was performed utilizing the Ion Torrent Proton (Thermo Fisher Scientific; Waltham, MA, USA). Briefly, RNA samples were depleted of ribosomal RNA using the Low Input RiboMinus Eukaryotic System v2 kit (Thermo Fisher Scientific). The cDNA library was then created with the ribosomal depleted RNA using the Ion Total RNA-Seq Kit v2 (Thermo Fisher Scientific). This included fragmentation via RNase III, hybridizing and ligating the RNA, performing reverse transcription, and amplification. Samples were labeled with the Ion Xpress RNA-Seq Barcode 1-16 Kit (Thermo Fisher Scientific) to enable multiplexing 4 samples per run. Templating, loading and sequencing were carried out using the Ion PI Template OT2 200 Kit v2, the Ion PI Chip Kit v2, and the Ion PI Sequencing 200 Kit v2 respectively (all from Thermo Fisher Scientific). Data was generated using the included Ion Reporter software (Thermo Fisher Scientific). Sequences were aligned to the mm10 mouse genome using the subread aligner [75] and counts were generated using the Bioconductor Rsubread package. Comparisons were performed using the Bioconductor edgeR package. Genes were identified as significantly different between groups if they had both an FDR adjusted p-value of 0.05 or less and an

absolute fold change of 1.5 or more. The full dataset has been deposited in the NCBI GEO Database under accession number GSE91398.

Quantitative RT-PCR analysis

cDNA was synthesized with the iScript Reverse Transcription Supermix kit (Bio-Rad; Hercules, CA, USA) using RNA from 4 FA Sham, 7 FA TAC, 4 DE Sham and 6 DE TAC hearts, each group including the 3 samples used in RNA-seq., and differential gene expression was validated by qRT-PCR using iTaq Universal Sybr Green Supermix (Bio-Rad). Primers used for validation were as follows: miR133a-2 F: 5'-GCCAAATGCTTTGCTGAAGCTG-3', miR133a-2 R: 5'-GCTGGTTGAAGGGGACCAAA-3', Ptprf F: 5'-CAACGATGGGCTCAAGTTCT-3', Ptprf R: 5'-TTCTTGGGCTTGTTCACCTC-3', Pamr1 F: 5'-CCCAGGAAAGAAGGAAGTGG-3', Pamr1 R: 5'-GGCAGCTCTTGCAGTTTTCA-3', 18S F: 5'-GGACAGGATTGACAGATTGATAG-3', 18S R: 5'-ATCGCTCCACCAACTAAGAA-3'. Samples were cycled at 95°C - 15 seconds, 60°C - 1 minute for 40 cycles. Samples were run on the 7900HT Fast Real-Time PCR System (Applied Biosystems; Waltham, MA, USA). Expression of Ptprf, miR133a-2 and Pamr1 was normalized to the ribosomal RNA 18S. Statistical analysis was carried out using two-way ANOVA for comparison of expression values, and linear regression for comparison of expression value to ventricle weight.

Assessment of candidate gene expression in human heart failure samples

To determine whether the identified candidate genes demonstrate differential expression in human heart failure, we examined their expression patterns in a published human nondiabetic heart failure and control myocardial biopsy dataset [76] available through the NCBI GEO database (GSE26887). Statistically significant differences in gene expression were determined by one-way ANOVA with Bonferroni correction.

Isolation of neonatal cardiomyocytes

Upon birth, neonatal hearts were harvested, trimmed of surrounding vascular and atrial tissue, and dissociated as previously described [77, 78]. Dissociation was performed using 1mg/mL Liberase TH (Roche; Pleasanton, CA, USA) in 1X HBSS by incubating hearts at 37 degrees for 5 minutes in solution, with pipetting to release cells after incubation. Media containing released NCMs was adjusted to 20% FBS-DMEM, and cellular dissociation was continued until the majority of cells were released. Cells were then filtered using a 70μm sieve, re-eluted in 20% FBS-DMEM with 20μm Ara-C and incubated at 37 degrees for 1 hour to allow fibroblasts to attach onto the plate. After incubation, media with suspended cardiomyocytes was carefully removed, spun and purified cardiomyocyte pellets were collected and frozen at -80°C.

DNA isolation and targeted bisulfite sequencing

DNA was isolated from purified neonatal cardiomyocytes of 8 DE- and 6 FA-exposed p0 mice using the Qiagen DNeasy Blood and Tissue Kit (Qiagen) according to the manufacturer's protocol. DNA was bisulfite converted using EpiTect Fast Bisulfite Conversion kit (Qiagen) according to the manufacturer's protocol. Converted DNA was amplified using HotStarTaq Master Mix (Qiagen), activated at 95°C for 15 minutes, cycled at 94°C – 30 seconds, 63°C – 45 seconds (-1°C/cycle for the first 10 cycles), 68°C – 1min for 10 cycles, for 40 cycles. The following primers were used, targeting the regions boxed in red shown in Figure 2.2:
GM6307 Promoter F: 5'-GTATTGGGTTTTGTTAAAAATAGTAGG-3', R: 5'-CCTCACCTTAATAATTCTTATATACCC-3', GM6307 Exon 1.1 F: 5'-GGGTATATAAGAATTATTAAGGTGAGG-3', R: 5'-CAAAACCCAACTACACACCTTAC-3', GM6307 Exon 1.2 F: 5'-GTAGGAGGGTTGGGGGAA-3', R: 5'-CAACCAACTAAAAAAAACTCACC-3', Ptprf CpG17 F: 5'-GTATTTGGTTTAGTTTTTGGATGTG-3', R: 5'-CAAACTCTACTCTTCTCCTCAATAC-3', Ptprf CpG24 F: 5'-TTTTTAGGTGTTGTAAAGGAAGTTTAAT-3', R: 5'-TACACTATTCTAAACCCTAACAAAC-3', Ptprf CpG79.1 F: 5'-ATTGGAAAGGGAGAGAAATTTA-3', R: 5'-CCCCCRTACAAAATTTCCC-3', Ptprf CpG79.2 F: 3'-GGGAAATTTTGTAYGGGGG-5', R: 3'-CCTACAACTCCACTCCTCTACAAAC-3', Pamr1 Promoter F: 5'-GGTTTTAGTTAGTGTTGTTTGTTATA-3', R: 5'-

AACTCTCCCACCCTCAACTAAAA-3', Pamr1 Exon 1 F: 5'-TTTTAGTTGAGGGTGGGAGAGTT-3', R: 5'-CAAAAAACTCCTAATCACTAACAATAC-3'.

Bisulfite converted DNA was sequenced in the University of Washington Northwest Genomics Center, using an Illumina MiSeq (Illumina; San Diego, CA, USA) in paired end mode, with a 250 bp read length. Samples were sequenced to a mean depth of approximately 0.5 million reads. Adapter sequences as well as low quality bases were removed from the raw reads using Trimmomatic (version 0.32) [79]. Briefly, we removed Illumina TruSeq3 adaptors, then excluded any bases on either end of the read with a quality score < 3, and finally used a moving window approach to trim off any portion of the read in which the average quality score over a four base moving window dropped below 15. Any reads < 36 bp in length after trimming were excluded. We then aligned trimmed reads against the mouse mm10 genome using the Bismark aligner (version 0.15.0) [80] in conjunction with the bowtie aligner (version 0.12.8) [81]. The trimming process results in a set of reads that remain paired, and sets of reads that are unpaired (because the matching pair is missing or was excluded). We aligned the paired and unpaired reads separately, then combined the resulting BAM files prior to extracting methylation calls using Bismark's methylation_extractor function.

We read the per-base methylation calls from Bismark into R using the Bioconductor bsseq package [82]. To minimize low quality methylation calls, we excluded any CpG with a read coverage < 5 in more than half of the samples.

Individual CpG methylation estimates are known to be highly variable, so we smoothed the methylation estimates over adjacent bases, by computing a moving average of all CpG sites within a 100 base moving window. We then made comparisons between groups at each CpG site using the Bioconductor DSS package [83]. Briefly, we model the smoothed methylation estimates (at each CpG) based on the Beta-Binomial distribution, estimating the dispersion parameter using a Bayesian hierarchical model. We then computed a Wald statistic for each CpG site. Our goal was to find genomic regions that appeared to be consistently differentially methylated between the DE and FA mice. We defined a differentially methylated genomic region based on several criteria; the region had to be at least 50 bp long, contain at least 3 CpGs, and at least 50% of the CpGs had to have a Wald p-value < 0.01.

2.3 RESULTS

Transcriptional profiling by RNA-seq reveals candidate target genes in the heart induced by in utero diesel exposure.

Table 2.1 shows the various comparison groups, the number of candidates identified by unadjusted p values less than 0.05 and then those identified after multiple hypothesis correction controlling for a false discovery rate. The number of genes differentially expressed (FDR < 0.05 and an absolute fold change > 1.5) after TAC are 880 in the DE exposed groups and 432 in the FA exposed groups. In contrast, the number of genes differentially expressed

after DE exposure are 5 in the sham group and 2 in the TAC group. These findings indicate that the magnitude of the TAC effect is much greater than that of the DE effect. Since gene expression after TAC has been studied extensively [84], we have focused primarily on genes affected by DE and will not discuss genes induced by TAC any further.

Table 2.2 shows the 5 genes that are differentially expressed in the DE and FA groups after sham operation. Three of the genes*, Gm8841*, *Pcdh1* and *Bbip1*, showed reduction in expression after DE exposure, while the remaining two, *Mir133a-2* and *Gck*, showed increased expression. Table 2.3 shows the 2 genes that were differentially expressed in the DE and FA groups after TAC surgery. *Ptprf* demonstrates increased expression, while *Pdk4* shows reduced expression. Table 2.4 lists genes identified in the interaction comparison, which identifies genes that respond differently to TAC, depending on exposure. These genes include protein tyrosine phosphatase, receptor type, F (*Ptprf*; also known as leukocyte common antigen related, LAR, phosphatase), *Mir133a-2* and peptidase domain containing associated with muscle regeneration 1 (*Pamr1*).

Further validation of individual candidate gene expression from the interaction group by qRT-PCR revealed interesting patterns of gene expression. Based on their statistically significant differences in expression across all 4 surgery and exposure conditions, we conclude that these candidates are most likely to be important in mediating the DE-induced susceptibility to heart failure. Expression of *miR133a-2* showed divergent regulation in adult hearts after exposure to DE *in utero*. DE mice undergoing sham surgery had elevated

expression compared to FA controls, but TAC surgery induced a marked suppression of expression while FA exposed animals showed induction of expression (Fig. 2.3A). Reduced expression of *miR133a-2* after TAC is associated with worse heart failure and fibrosis. These findings are consistent with the previously reported role for miR133a-2 in functioning to suppress pathological cardiac hypertrophy and fibrosis [85, 86].

Expression of *Ptprf* was not significantly changed by DE in mice undergoing sham surgery. In mice undergoing TAC, those exposed to DE *in utero* showed an increase in expression compared to those exposed to FA (Fig. 2.3C). This elevated expression is associated with worse heart failure and cardiac fibrosis, and is consistent with a causal role for PTPRF in promoting pathological hypertrophy and heart failure.

The expression of *Pamr1* was also increased resulting from exposure. *Pamr1* expression is increased in both FA and DE exposed mice after TAC, though the increase is larger in the DE cohort. Expression of *Pamr1* also showed a significant correlation with the ventricular weight to tibia length ratio (Fig. 2.3E). This elevated *Pamr1* expression, like that of *Ptprf*, is associated with worse heart failure and cardiac fibrosis, and is also consistent with a causal role for *Pamr1* in promoting pathological hypertrophy and heart failure.

Ptprf, miR133a-2 and Pamr1 gene expression are altered in a human heart failure gene expression dataset

To determine whether these identified target genes demonstrate altered expression in human heart failure, we examined their expression in a publicly available Affymetrix dataset (NCBI GEO database: GSE26887) derived from human myocardial biopsies taken from patients with non-diabetic heart failure or control hearts [76]. *Mir133a* expression is reduced in both forms of heart failure, consistent with a role in protecting against heart failure. Examination of *Ptprf* and *Pamr1* expression, however, indicates that both genes show significant increases in expression in non-diabetic heart failure when compared to controls (Fig. 2.4). These expression patterns are consistent with a role for these genes in contributing to human heart failure.

DNA methylation patterns at the Ptprf, Pamr1 and miR133a-2 loci

In our model of DE-related heart failure, exposure to DE occurs only during gestation, with no exposure after birth, yet these mice develop significantly worsened heart failure as adults after TAC. This suggests that long-lasting epigenetic modifications, such as DNA methylation, are responsible for this susceptibility. To test this, we performed targeted bisulfite sequencing at CpG islands and promoter regions associated with *Ptprf*, *miR133a-2* and *Pamr1* from neonatal cardiomyocytes of mice exposed to FA or DE *in utero*. We found that while *in utero* DE exposure did not induce significant differences in DNA methylation in either the *Pamr1* or *Ptprf* loci (data not shown), the first exon of GM6307, the gene in which *miR133a-2* resides, had decreased methylation based on the criteria discussed above and in the legend for Fig. 2.5. This finding

is consistent with the elevated expression of *miR133a-2* in hearts from mice exposed to DE in the sham surgery group (Fig. 2.3A).

2.4 DISCUSSION

We have shown that gene transcription is significantly altered in mice as result of *in utero* DE exposure and adult TAC surgery. We identified the genes *Ptprf*, *miR133a-2* and *Pamr1* as being differentially regulated and verified these findings by qRT-PCR. To the best of our knowledge, these genes have not been previously identified as being responsive to diesel exhaust exposure in the heart. While the exposure level used in this study (300 ug/m^3) is well above the 2015 national average for the United States (8 ug/ m^3), countries such as Egypt and Saudi Arabia have averages around 100 ug/m^3 [87], and in 2013 Beijing reached a record of almost 1,000 ug/m^3. Additionally, occupational exposure is of great concern. One study showed that workers in high exposure settings, such as tunnel construction, can receive exposures up to 400 ug/m^3 $PM_{2.5}$ [88], and steel plant workers can reach exposure levels above 1200 ug/m^3 PM_{10} [63]. Our exposure levels in this study thus reflect real world human exposure.

PAMR1 has been postulated to play a role in the regeneration of skeletal muscle based on its expression pattern [89], to play a role in the acute insulin response to glucose [90] and to be suppressed by promoter methylation in breast cancer [91]. To the best of our knowledge, no functional studies have been published and a role for PAMR1 in cardiac hypertrophy and heart failure has not been reported. It is unclear whether these changes in gene expression have

individual roles in the development of DE-induced heart failure, or if the combination of these gene changes is required. The expression pattern indicates that increased expression is associated with increased cardiac hypertrophy and fibrosis.

PTPRF and other tyrosine phosphatases play critical roles in mediating signal transduction by limiting intracellular phosphorylation cascades that occur following the autophosphorylation of receptor tyrosine kinases [92, 93]. Overexpression of *Ptprf* has been shown to limit insulin sensitivity and thus promote insulin resistance in mouse models, while knockdown enhances insulin sensitivity in cultured cells [94-96]. Common single nucleotide polymorphisms in *Ptprf* are associated with the development of coronary artery disease in type 2 diabetic patients [97]. Previous work has shown using *in vitro* models that *Ptprf* expression is decreased following treatment with tumor necrosis factor α (TNFα), and that *Ptprf* expression is readily modified to regulate cell signaling [98]. To the best of our knowledge, PTPRF has not previously been associated with the development of heart failure. Based on its expression pattern, we hypothesize that exaggerated expression in hearts after in utero DE exposure likely either potentiates pathological hypertrophic signaling or limits antihypertrophic signaling.

A role for miR133a in cardiac hypertrophy is better established. *miR133a-2* encodes a premature form of miR133a, which controls cardiac development [99]. Reduced expression of miR133a leads to enhancement of cardiac hypertrophy *in vitro* by increased expression of its target IP(3)RII [100].

Overexpression of miR133a in the heart has been reported to suppress cardiac fibrosis but not cardiac hypertrophy after transverse aortic constriction [86], which is consistent with our results. MiR133a loss of function has previously been associated with myocyte apoptosis after ischemia-reperfusion through increased expression of caspase 9 [101] and skeletal muscle myopathy through an effect on its target dynamin 2 [102]. DNA hypermethylation of a CpG island associated with the miR133a-2 cluster and reduced *miR133a-2* expression have been associated with colorectal cancer [103]. In comparison, our results show that *in utero* DE resulted in a ~2 fold increase in *miR133a-2* expression at baseline in our sham-operated mice (Table 2.2 and Figure 2.3A). Our previously reported baseline phenotypic assessment in sham-operated mice did not reveal *in utero* DE exposure to have any effect on cardiac function or myocyte hypertrophy [16]. We observed this increased *miR133a-2* expression to be downregulated following TAC in the *in utero* DE-exposed mice (Table 2.1 and Figure 2.3A), with a simultaneous increase in LV wall thickness, fibrosis, and decreased fractional shortening, as previously reported [16]. This downregulation of *miR133a-2* with concomitant exacerbation of heart failure with reduced ejection fraction may suggest that the increased *miR133a-2* expression at baseline played a protective mechanism in preserving cardiac function, and that loss of this increased expression results in the exacerbation of heart failure. Our DNA methylation studies in neonatal cardiomyocytes reveal hypomethylation within the first exon of *GM6307*, which is consistent with our observation of increased *miR133a-2* expression in the baseline sham-operated mice. The loss of increased *miR133a-*

2 expression in the *in utero* DE-exposed mice in heart failure may imply that there may be dynamic modifications of DNA methylation or multifactorial changes in chromatin assembly and transcription factor accessibility that are modified by *in utero* DE exposure. These observations suggest that the baseline hypomethylation and increased *miR133a-2* expression at baseline is an advantageous adaptation, but that the dysregulation of its expression in heart failure is uniquely affected by *in utero* DE exposure. The loss of *miR133a-2* overexpression in DE-exposed hearts after TAC may facilitate pathological hypertrophy by enhanced IP(3)RII signaling and increased apoptosis mediated by caspase 9 [100].

The effect of environmental toxicant exposure on cardiac hypertrophy via regulation of *miR133a* expression and DNA methylation has been previously reported [104]. Exposure to the polycyclic aromatic hydrocarbon (PAH), phenanthrene, causes cardiac and myocyte hypertrophy in both *in vivo* and *in vitro* models. In male Sprague-Dawley rats and the H9C2 rat cardiomyoblast cell line, phenanthrene exposure was associated with a decrease in *miR133a* expression and a simultaneous increase in protein levels of important miR133a cardiac hypertrophy targets Cdc42 and RhoA. This decrease in *miR133a* expression was associated with an increase in DNA methylation at 5 CpG sites located near the putative transcription start site of *miR133a* in H9C2 cells. Overexpression of *miR133a* via transfection of *miR133a* mimetics, or inhibition of DNA methylation with a DNA methylation inhibitor (5-aza-2'-deoxycytodine), largely eliminated the hypertrophic effect of phenanthrene. PAHs are a significant

component of diesel exhaust particulate mass and we have previously reported our diesel exhaust exposure system to generate DE with a mass fraction of particle-bound PAH at 20 ng/μg [52]. Phenanthrene is a major constituent of environmental PAHs and has been reported to be a significant component of diesel exhaust [105], perhaps suggesting that PAHs including phenanthrene may contribute to our observed effects on heart failure and DNA methylation. Although we observed *in utero* DE exposure to result in altered *miR133a-2* expression in a manner similar to that reported previously [104], our observed DNA methylation results of hypomethylation of the first exon are in contrast and perhaps suggests a unique epigenetic mechanism of action in *in utero* diesel exhaust-induced adult susceptibility to heart failure.

One surprising finding of our work is that relatively few genes are significantly affected in the heart after *in utero* DE exposure, but we believe that this finding is likely due to dilutional effects from using whole heart RNA. Future studies using adult cardiomyocyte RNA-seq would likely generate additional candidate genes. Another unaddressed question is the effect of *in utero* DE exposure on the global DNA methylation pattern in cardiomyocytes. We have attempted to perform genome wide BS-seq in whole adult heart DNA, but to date no differentially methylated regions have been consistently identified, likely due to the dilutional effect of non cardiomyocytes. Previous studies of methylation in adult cardiomyocytes have relied on purification of adult cardiomyocytes [106]. A future study analyzing DNA methylation patterns in isolated adult cardiomyocytes will address this question.

Another potential caveat with studying whole heart RNA is that gene expression changes may reflect a shift in cell population rather than a change in expression within a given cell type. We do not favor this hypothesis as both *miR133a-2* and *Pamr1* are expressed predominantly in muscle tissue (30, 33) and the relative contribution of additional cells such as inflammatory cells is still likely to be modest compared to cardiomyocytes and fibroblasts.

Though it has been shown in multiple studies that exposure to $PM_{2.5}$ is associated with changes in DNA methylation [62, 63, 70], the mechanism is unclear. In our study, we initially assessed whether the DNA methylases DNMT1, DNMT2 or DNMT3 were differentially expressed by qRT-PCR, but did not see any significant difference, which is consistent with our RNA-seq data (data not shown). It has been shown that exposure to diesel exhaust increase reactive oxygen species (ROS) production [107, 108], which can in turn interact with DNA to oxidize methylcytosine (mC) to hydroxymethylcytosine (hmC). hmC has been shown to prevent methyl-binding proteins (MBP) from binding to methylated cytosines [109]. This inability of MBP binding can prevent the normal chromatin silencing that would occur at these sites, allowing for transcriptional expression. Furthermore, oxidation to hmC has been shown itself to be an intermediary to the potential loss of DNA methylation [110, 111]. In addition to the role of hmC as both a blockade of chromatin silencing and a stepping stone to loss of methylation, the guanine oxidative lesion 8-oxoguanine also can inhibit the binding of MBPs, preventing the silencing of chromatin regions [109]. Taken

together, these processes could explain the observations of changes in DNA methylation associated with exposure to DE.

The findings of decreased DNA methylation at the first exon of GM6307 are intriguing as it gives credence to the idea that *in utero* exposure to DE affects the developing heart through altered epigenetic patterning. DNA methylation of the first exon has been shown to control gene regulation [112], and the decreased DNA methylation in DE-exposed mice does correlate with the higher expression observed in adults that have undergone sham surgery. The DE-exposed TAC surgery group shows a reduction in expression, however, which is not explained by our DNA methylation findings, and is perhaps due to other epigenetic modifications or altered signaling as a result of the surgery.

A limitation of our work is that these changes in gene expression represent associations and do not demonstrate causality. Our initial attempts to investigate effects of in utero DE exposure on TAC-induced heart failure in mice that overexpress miR133a in the heart were inconclusive because the WT FVB strain used to generate these mice is not susceptible to TAC-induced heart failure after in utero DE exposure (data not shown), in contrast to the C57BL/6 strain used in this study and previously reported studies (12). We also isolated neonatal cardiomyocytes from this strain after in utero DE exposure to assess whether cardiomyocytes from exposed animals were more susceptible to hydrogen peroxide induced apoptosis but did not observe increased susceptibility (data not shown). Furthermore, we overexpressed both miR133a and PTPRF in H9c2 myoblasts by lentiviral transduction, to assess whether stable changes in

expression of these genes affect susceptibility of these cells to hydrogen peroxide-induced apoptosis. Unfortunately, in our studies, these cells rapidly undergo necrosis and thus an effect of candidate gene overexpression on apoptosis could not be measured (data not shown). Future studies on genetically modified mice generated on a C57BL/6 background are required to truly assess the contribution of these genes to diesel exhaust induced susceptibility to heart failure, but are beyond the scope of the current study.

We have reported on significant transcriptional and DNA methylation changes associated with *in utero* DE exposure and adult TAC surgery. Further analysis of how these genes impact adult susceptibility to heart failure is in progress. Both gain- and loss-of-function models will be informative for the development of air pollution-associated heart failure treatments. miR133a has already been identified as a biomarker of patient outcome after valve replacement [113] and is currently being studied as a treatment post-infarction to improve patient outcome [114]. Determining whether miR133a can play a similarly protective role in our model of DE-induced heart failure, alongside the potential benefits of decreasing *Ptprf* and *Pamr1* expression, will pave the way for further drug development for patients with air pollution-associated heart failure.

Figure 2.1

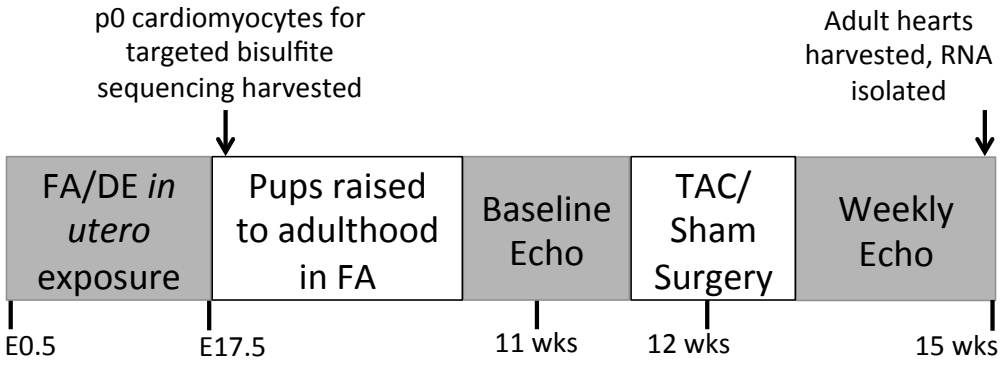

Exposure and sample collection scheme.

Figure 2.2

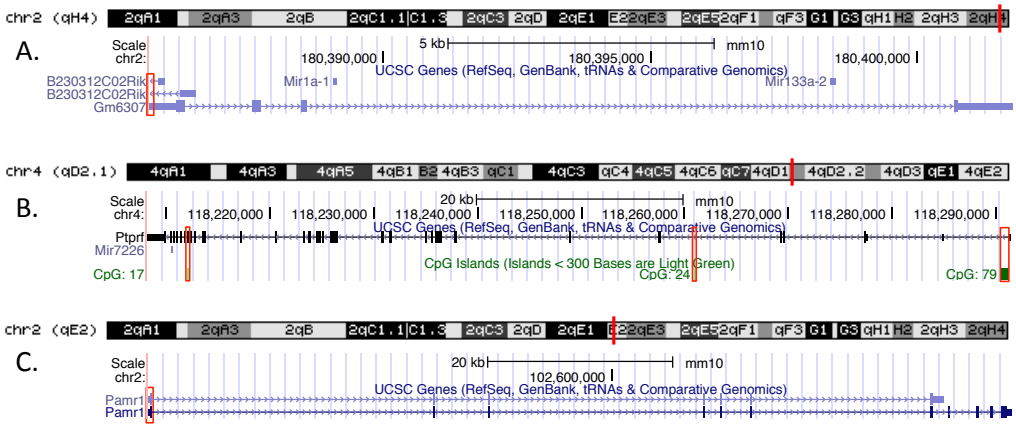

Genomic regions for bisulfite sequencing. Genomic regions highlighted in the red boxes are areas targeted for bisulfite sequencing. Targets correspond to A) GM6307 promoter and first exon, B) Ptprf CpG islands 17, 24 and 79, and C) Pamr1 promoter and first exon.

Figure 2.3

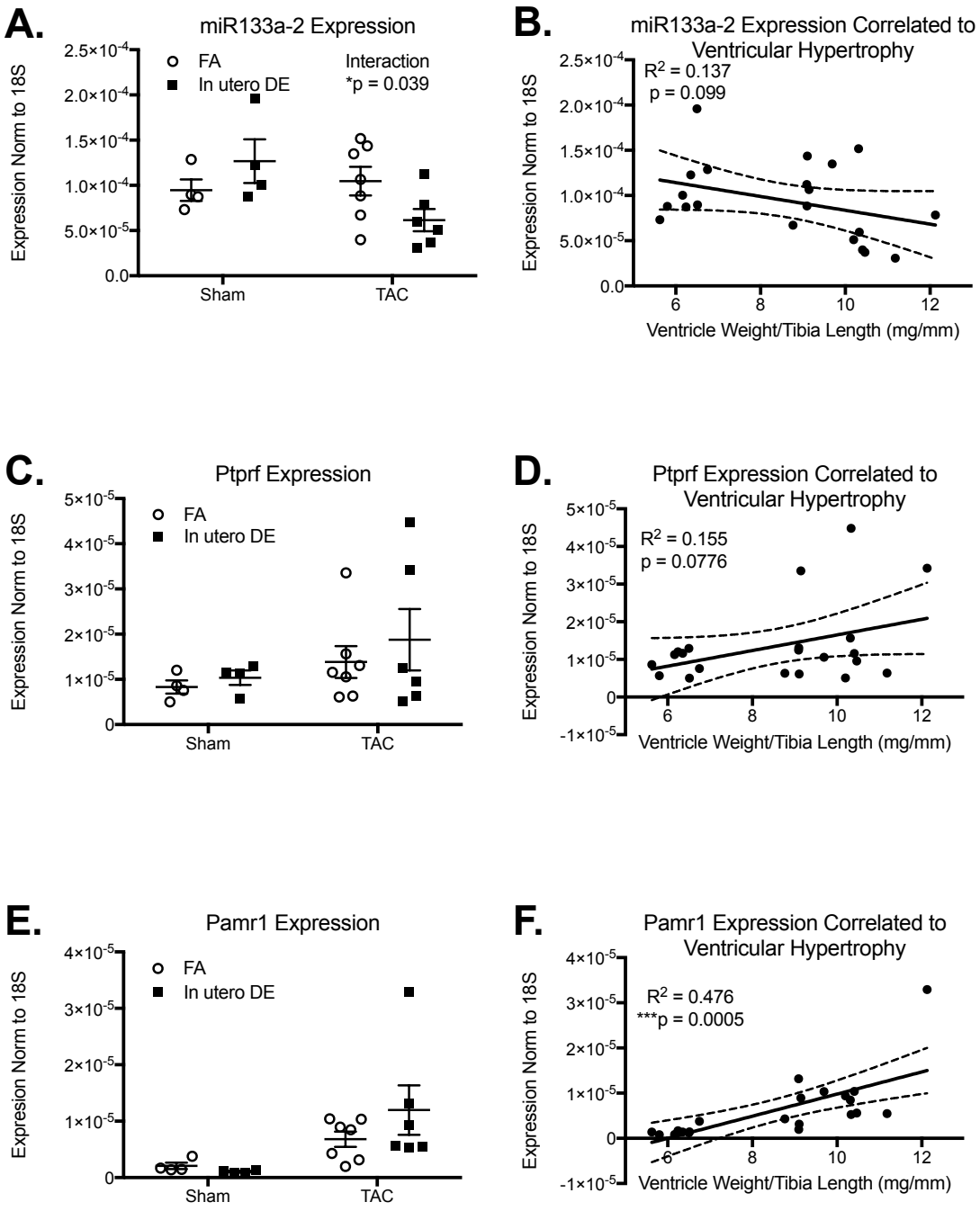

Expression of miR133a-2, PTPRF and Pamr1 after in utero DE exposure and TAC surgery, correlated with VW/Tibia Length measurements. A, C and E show the ddCT values for miR133a-2, Ptprf and Pamr1, respectively, in the four categories: FA Sham, DE Sham, FA TAC, DE TAC. B, D and F show the

corresponding linear regression, plotting expression as a function of ventricle weight normalized to tibia length. * indicates $p<0.05$.

Figure 2.4

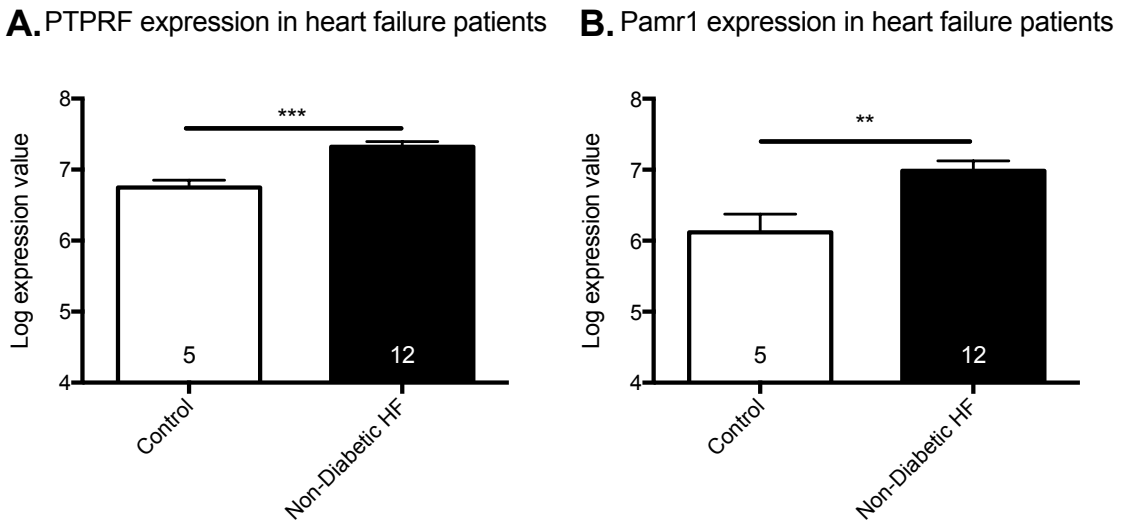

Expression of A. Ptprf and B. Pamr1 in human heart failure samples. Significance calculated using One-way ANOVA with post-hoc Bonferroni. ** indicates $p<0.005$, *** indicates $p<0.0005$. Data is derived from publicly available Affymetrix dataset (NCBI GEO database: GSE26887).

Figure 2.5

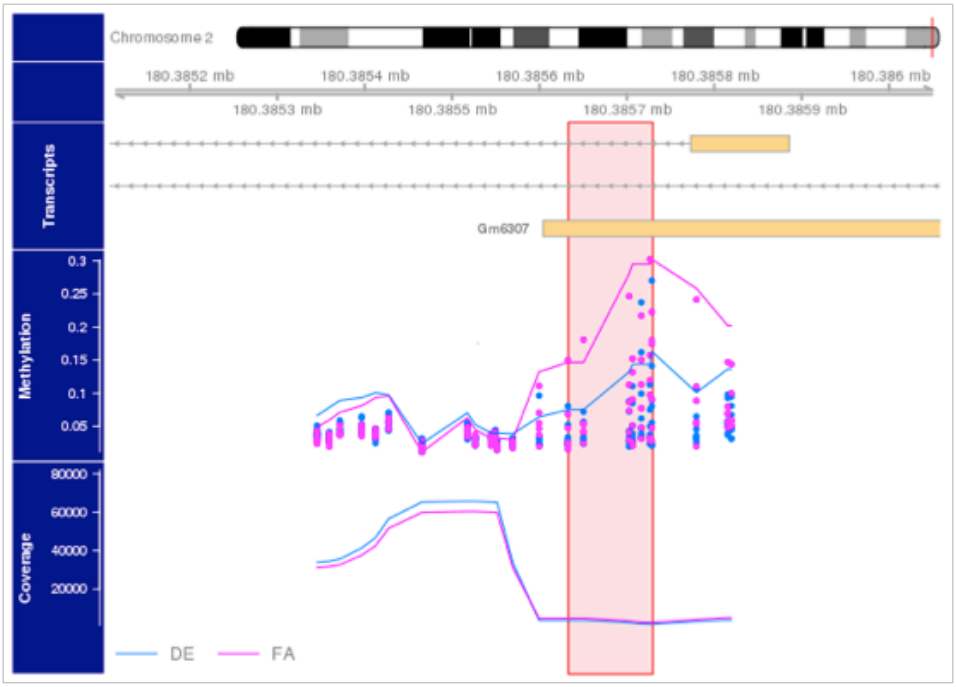

Targeted bisulfite sequencing of GM6307 promoter and exon 1. The upper portion of the plot contains a karyogram of Chromosome2, with a vertical red bar showing the region of interest; the horizontal bar just below the karyogram shows the ‘zoomed in’ region of the chromosome that we are inspecting. The transcripts portion of the plot presents UCSC genome browser-style transcripts, where the orange bars represent exons, and the grey lines represent introns. The arrows in the intronic region represent the direction of transcription. Below that we present the observed (individual points) and smoothed (lines) % methylation estimates for the CpGs in this genomic region. Pink points and lines represent FA samples, and blue represent DE samples. In the lowest (Coverage) portion of the plot we present the sequencing read depth (e.g., the number of sequencing reads that aligned over each CpG). The pink vertical bar indicates the genomic region that

appears to be differentially methylated. This region spans 96 bp, and contains 7 CpGs, all of which indicate a decrease in methylation in DE exposed animals at a Wald p-value < 0.01.

Table 2.1. Number of genes that were altered in expression due to exposure, surgery type or interaction.

Comparisons	**Unadjusted P<0.05**	**FDR<0.05**
DE TAC vs DE Sham	1375	880
DE Sham vs FA Sham	316	5
DE TAC vs FA TAC	153	2
FA TAC vs FA Sham	931	432
Interaction	321	3

Table 2.2. Top 5 specific genes induced by DE in sham operated animals (i.e. DE Sham vs FA Sham)

Gene Symbol	**LogFC**	**P Value**	**FDR**
Gm8841	-1.140	3.33e-08	0.000344
Pcdh1	-0.895	6.97e-07	0.002490
Bbip1	-1.130	7.24e-07	0.002490
Mir133a-2	1.970	1.21e-05	0.027200
Gck	1.180	1.32e-05	0.027200

Table 2.3. Specific genes induced by DE in TAC operated animals (i.e. DE TAC vs FA TAC)

Gene Symbol	**LogFC**	**P Value**	**FDR**
Ptprf	1.580	6.09e-08	0.000628
Pdk4	-1.100	1.25e-06	0.006440

Table 2.4. Specific genes showing a differential response to TAC, depending on exposure (i.e. interaction)

Gene Symbol	**logFC**	**P Value**	**FDR**
Ptprf	-2.380	2.29e-08	0.000236
Mir133a-2	3.120	6.64e-07	0.003430
Pamr1	-2.630	4.03e-06	0.013900

Chapter 3

In utero exposure to diesel exhaust particulates is associated with altered neonatal transcription and metabolism

3.1 INTRODUCTION

Exposure to particulate matter air pollution has shown to have an association with increased incidence of cardiovascular disease [6, 68, 69], including arrhythmias [8], myocardial infarction [69] and heart failure [115]. Prenatal and early-life exposure to $PM_{2.5}$ and PM_{10} is associated with deleterious effects, such as decreased placental mitochondrial DNA [30], decreased fetal growth [43] and birth weight [42] and increased newborn systolic blood pressure [45]. Currently, understanding the effect of *in utero* on newborn and early life health has become of great concern, as studies are beginning to show evidence of maternal exposure to air pollution and offspring risk of congenital heart defects [48, 49] and childhood cancers such as retinoblastoma and acute lymphoblastic leukemia [116], as well as increased incidence of maternal gestational type 2 diabetes mellitus [117], which can in turn increases infant risk of metabolic and cardiac disorders [118]. Our lab has shown that *in utero* exposure to DE in mice predisposes the offspring to an increased susceptibility to heart failure after TAC surgery [16].

We have previously discovered transcriptional dysregulation in the hearts of adult mice exposed *in utero* to DE (Chapter 2)[119]. This led to questions about whether this *in utero* exposure is altering the transcriptional profile

specifically within the cardiomyocytes of these mice. To hone in on the early changes that might underlie the previously observed later life susceptibility to heart failure, RNA-sequencing was performed on whole hearts and isolated cardiomyocytes from p0 neonatal pups. We observed a large number of transcriptional changes associated with only *in utero* exposure to DE, many of which are involved in normal cardiac metabolism. We have also determined the baseline metabolic phenotype of both neonatal cardiomyocytes and mitochondria isolated from adult hearts to establish the potential role of metabolic dysregulation in our model of *in utero* DE exposure and increased adult susceptibility to heart failure after TAC.

3.2 METHODS

Diesel exhaust exposure and mice

Exposure conditions were carried out as described in Chapter 2.2. Female mice were paired with male mice for timed mating in FA. After observation of a vaginal plug, pregnant mice were put into FA or DE with exposures beginning at E0.5 and lasting until E17.5, at which point pregnant mice were transferred from the Northlake facility to the UW Medicine South Lake Union SPF vivarium for neonatal sample collection or weaned and kept until 11-12 weeks for adult sample collection.

Isolation of NCMs and mitochondria

Isolation of NCMs was carried out as described in Chapter 2.2. Mitochondria were isolated from adult hearts following a published protocol [120]. Hearts were removed, trimmed of vascular and atrial tissue, and washed in mitochondrial isolation medium (MIM) (0.3 M sucrose, 10 mM sodium HEPES, pH 7.2, and 0.2 mM EDTA). A small (15-20 mg) piece of tissue was removed and snap frozen for separate analysis. The remaining heart was minced, trypsin-digested (0.125 mg/mL) for 15 minutes on ice, and the reaction was stopped by addition of MIM containing 1 mg/mL BSA and 0.65 mg/mL trypsin inhibitor. The samples were then spun at 1500g at 4°C for 1 minute and the supernatant was removed. The samples were resuspended in MIM containing BSA, and homogenized with a Teflon-glass homogenizer. The samples were then spun at 800g at 4°C for 10 minutes, and the supernatant was transferred to a fresh tube and pelleted at 8000g at 4°C for 15 minutes. The pellet was washed in cold MIM twice, and resuspended in a final volume of 100 µL MIM.

RNA sequencing

RNA was purified from frozen p0 isolated NCMs using Trizol (Thermo Fisher Scientific, Waltham, MA, USA), following the manufacturer's protocol. Ribosomal RNA was depleted by poly-A enrichment, and sample libraries were created using the TruSeq Stranded mRNA kit (Illumina, San Diego, CA). Each library was barcoded using the Illumina adapters, and amplified with 13 cycles of PCR. Library concentrations were quantified using the Quant-it dsDNA Assay

(Life Technologies, Carlsbad, CA). Libraries were normalized and pooled based on Agilent 2100 Bioanalyzer results (Agilent Technologies, Santa Clara, CA), and the pools were sequenced on an Illumina HiSeq 2500.

To process sequences, Illumina RTA-generated BCL files were converted to FASTQ files and sequence read and base quality were checked using the FASTX-toolkit (http://hannonlab.cshl.edu/fastx_toolkit/) and FastQC (http://www.bioinformatics.babraham.ac.uk/projects/fastqc/). Sequences were aligned to mm10 with reference transcriptome Ensembl v67 using Tophat [121]. Lane level bam data files were merged using the Picard MergeSamFiles tool and suspected PCR duplicates were marked, not removed, in the alignment files using the Picard MarkDuplicates tool (http://broadinstitute.github.io/picard/). Local realignment was performed around indels, and base quality score recalibration was run using GATK tools [122]. Variant detection was performed with the GATK Unified Genotyper version 2.6.5 [123], and aligned data were used for isoform assembly and quantitation with Cufflinks [121, 124]. Fragment counts were generated using the featureCounts function in the Bioconductor Rsubread package [75]. Comparisons were performed using the Bioconductor edgeR package. Genes were identified as significantly different between groups if they had a 25% or greater difference in expression between the two groups at an FDR adjusted p-value of 0.05 or less.

Metabolic activity analysis

Cellular respiration was performed on NCMs using the mitochondrial

stress test (Agilent; Santa Clara, CA, USA), measured using a Seahorse XFe24 extracellular flux analyzer (Agilent). NCMs were plated on provided 24 well plate coated in fibronectin, plating 3-4 replicates per samples, and cultured for 3 days in 20% FBS-DMEM with 20 μM Ara-C. On the day of measurement, cells were washed with XF assay medium (Agilent) supplemented with 25 mM glucose, 1 mM sodium pyruvate and 2 mM L-glutamine, and replenished with the same media and incubated at 37°C without CO_2 an hour prior to measurement. Injection scheme is represented in Fig. 3.1A, with concentrations at 1.5 μM oligomycin, 1 μM FCCP, 1 μM Rotenone and 1 μM antimycin A. Calculations for values represented in Fig. 3.1 were done by B. subtracting the non-mitochondrial respiration (minimum rate after AMA/Rot injection) from last baseline measurement prior to oligomycin injection, C. subtracting the non-mitochondrial respiration from maximum rate after FCCP injection, D. Subtracting the minimum rate measured after oligomycin injection from last rate measured before injection, E. Subtracting the basal respiration from the maximal, and F. Dividing the ATP production rate by the basal respiration rate, multiplying by 100 to show as a percentage. Normalization to μg DNA/well was performed by phenol:chloroform extracting DNA from each well, and measuring DNA concentration using the Quant-iT PicoGreen dsDNA assay kit (Thermo Fisher Scientific), following the manufacturers protocol. Statistical comparisons were performed using a t-test between the measurements made in male DE vs. FA NCMs (n=7, n=8 respectively).

Mitochondrial respiration rate was measured using an Oxygraph-2 k

system (Oroboros; Innsbruck, Austria), monitored at 37°C. Roughly 0.1 mg/mL of the mitochondrial prep was injected into the chamber containing 2 mL of Buffer Z (105 mM K-MES, 30 mM KCl, 5 mM KH_2PO_4, 5 mM $MgCl_2$-$6H_2O$, and 0.5 mg/mL Bovine serum albumin, pH 7.1). Oxygen levels were calibrated, and a final concentration of 2 mM malate was injected. For state 4 respiration, either 5 mM of pyruvate and 10 mM of glutamate (complex I respiration, or cI) or 20 μM of palmitoyl-L-carnitine (fatty acid oxidation, or fao) was injected. For state 3 respiration, 2.5 mM ADP was added to ensure saturation. 6 μM of cytochrome C was injected to detect level of mitochondrial damage (no significant difference between FA and DE, data not shown). 10 mM of succinate was injected (complex II respiration, or cII), followed by mitochondrial uncoupling using injections of FCCP at 0.05 μM increments until respiration began to fall. Complex I respiration was inhibited with injection of 0.5 μM rotenone, and all mitochondrial respiration was inhibited with injection of 2.5 μM antimycin A. Results were normalized to protein concentration of the mitochondrial preps. Protein was measured using a BCA assay (Thermo Fisher Scientific; Waltham, MA, USA) to manufacturer's protocol. Non-mitochondrial respiration was subtracted from all measurements, and statistical comparisons were performed using a t-test between the measurements in male DE vs FA mitochondrial (n=5, n=8 respectively)

Mitochondrial copy number analysis

The mitochondrial copy number of samples was determined by qPCR, following a published protocol [125]. DNA was isolated from frozen p0 NCMs and

adult heart pieces using the Qiagen DNeasy Blood and Tissue kit (Qiagen, Germantown; MD, USA), following the manufacturer's protocol. Amplifications were performed using the mitochondrial primers mMitoF: 5'-CTAGAAACCCCGAAACCAAA-3' and mMitoR: 5'-CCAGCTATCACCAAGCTCGT-3' and the genomic primers mB2MF: 5'-ATGGGAAGCCGAACATACTG-3' and mB2MR: 5'-CAGTCTCAGTGGGGGTGAAT-3'. Samples were run on the 7900HT Fast Real-Time PCR System (Applied Biosystems; Waltham, MA, USA), cycling at 95°C - 15 seconds, 60°C - 1 minute for 40 cycles, and quantification was performed using a prepared standard curve ranging from 10^2-10^8 copies/µL. Statistical significance was determined using a t-test between ratios measured in male DE vs FA samples (In neonatal samples, n=4, n=6 respectively, in adult samples n=5, n=8 respectively).

3.3 RESULTS

In utero exposure to DE results in altered transcriptional profiling

To assess alterations in transcription due to *in utero* exposure to DE, RNA-seq was performed on isolated NCMs from FA and DE p0 pups. We identified 300 transcripts that were significantly differentially expressed between FA and DE exposure. Table 3.1 shows the top ten genes with differential expression between exposure groups. Table 3.2 shows the top ten pathway hits using Qiagen's Ingenuity Pathway Analysis, with arrows indicating the direction

of expression change for genes identified as altered. In both, we can see a clear link to exposure and altered transcription of metabolic genes, showing a consistent decrease in expression in the DE NCMs.

In utero exposure to DE alters neonatal cardiomyocyte oxygen consumption

To determine whether the transcriptional changes identified in Tables 3.1 and 3.2 correlated to a functional change in the metabolic capacity of NCMs, we tested the rate of oxygen consumption of DE and FA NCMs using the Seahorse XFe24 Analyzer. However, since the switch from glucose oxidation to fatty acid oxidation in the neonatal heart doesn't occur until sometime between postnatal day 1-7 [126, 127], we tested the response of NCMs using pyruvate/glutamate to fuel oxygen consumption. Figure 1A shows the average oxygen consumption of each group at the three time points taken at baseline and after the injections of oligomycin, FCCP and antimycin A/rotenone. After subtracting the non-mitochondrial oxygen consumption, we found that both the baseline and maximal measurements are significantly lower in the DE NCMs (Fig. 1B and C). The ATP production and coupling efficiency of the DE NCMs was also found to be significantly lower than the FA NCMs (Fig. 1D and F). DE NCMs also demonstrated a lower spare respiratory capacity, though it was not statistically significant (Fig. 1E). Taken together, this indicates a decreased capacity for oxidative phosphorylation in DE NCMs.

In utero exposure to DE alters adult heart mitochondrial respiration

To determine whether the observed reduction in metabolic capability in neonatal cardiomyocytes persists to adulthood, we examined the mitochondrial respiration of isolated mitochondria from the hearts of 11-12 week old mice. Respiration was fueled by either pyruvate and glutamate, to determine whether the observed change in neonatal cardiomyocytes is maintained through growth, or palmitoyl-L-carnitine, to test whether the observed decrease in transcripts involved in fatty acid β-oxidation (Table 3.2) has a functional effect on adult metabolism. Mitochondrial oxygen consumption rate was measured in OROBOROS Oxygraph-2k high-resolution respirometry chambers.

Surprisingly, we observed an inversion of the findings in the neonatal cardiomyocytes, as state 4 respiration fueled by pyruvate/glutamate was significantly higher in the mitochondria from FA hearts (Fig. 3.2A), suggesting increased proton leak. While this did not have an effect on state 3 cI or cI+II-driven respiration (Fig. 3.2B,C), which is largely driven by substrate oxidation and ATP turnover, it did impact the respiration control ratio (RCR), which was significantly higher in the DE mitochondria (Fig. 3.2E), which is indicative of better function [128]. There was no observed change in maximal respiration (Fig. 3.2 D). When palmitoyl-L-carnitine was used as the fuel driving respiration, we observed no significant difference in FA and DE mitochondria (Fig. 3.3). Taken together, we found that while pyruvate/glutamate-driven oxygen consumption was decreased in DE NCMs, this phenotype either reversed itself by adulthood, or is due to non-mitochondrial effects of the cellular environment.

In utero exposure to DE increases cardiac mtDNA in adult mice

Given the findings of decreased metabolic activity in DE NCMs, we wanted to determine whether the mitochondrial load of the NCMs varied enough to explain the observed metabolic differences. However, there was no significant difference in mitochondrial load as determined by mtDNA copy number detected between FA and DE NCMs (Fig. 3.4A). Similarly, we tested the mitochondrial load of adult hearts after *in* utero exposure to DE, and observed a significant increase in mtDNA in the DE hearts (Fig. 3.4B).

3.4 Discussion

We have shown that the transcriptional profile of NCMs is significantly altered as a result of *in utero* exposure to DE, in large part affecting genes associated with metabolic pathways and cell cycle regulation (Tables 3.1, 3.2). Metabolic dysregulation is a hallmark feature of heart failure [129], with decreased fatty acid oxidation and increased glycolysis playing an important role in late-stage heart failure [130, 131]. While it is unclear how these findings might affect adult susceptibility to heart failure, multiple studies have discovered a link between exposure to air pollution and metabolic dysregulation [132-134]. Combined with our prior findings of increased expression of Ptprf (Chapter 2, Table 2.4, Fig. 2.3C,D), a transcriptional change associated with decreased sensitivity to insulin signaling [95], this suggests a potential role for metabolic dysregulation in our model of *in utero* DE exposure and adult susceptibility to heart failure.

Additionally, we have shown that respiratory capabilities of NCMs from *in utero* DE exposed neonates are hindered at both baseline and maximal respiration (Fig. 3.1B,C). While coupling efficiency was lower in DE NCMs (Fig. 3.1F), indicative of higher energy loss and ROS production [135], DE adult isolated mitochondria fueled by pyruvate/glutamate showed increased RCR (Fig. 3.2E), indicative of lower energy loss and ROS production [128]. One potential explanation for these findings is that DE cardiomyocytes acquire a compensatory increase in metabolic capability with age. An alternate explanation is that the shift in metabolic capability is due to cellular environment, rather than mitochondrial capability. To test this hypothesis, the metabolic phenotype of isolated mitochondria from NCM should be clarified; if the mitochondria of NCMs show no significant difference in the rate of oxygen consumption, then the cellular environment must be a major determinant in the metabolic capability of these cells. In adult mouse cardiac tissues, it is challenging to evaluate cellular respiration. While isolated mitochondria have the benefit of being easily extracted and are stable during experimental handling, the lack of cellular context remove important influences. Unfortunately, permeabilized cardiac fibers can lose cellular structure contributing to metabolism [136], as well as lose significant mitochondrial populations [137], making them less suitable to *in vitro* study, though homogenized cardiac tissue has shown promise [137]. To follow up on these experiments, testing the respiratory capabilities of both the isolated mitochondria of NCMs and homogenized cardiac tissue would be recommended.

The finding of increased mtDNA copy number in the adult heart is particularly intriguing, as it would suggest that the hearts might be overall more metabolically active. Traditionally, it has been shown that heart failure is associated with a decrease in mtDNA copy number [138-140], but this is often associated with end-stage heart failure. It is unclear how increased mtDNA copy number may affect early heart failure, as some studies have shown that exposure to cardiotoxic drugs can actually increase the mtDNA copy number. Exposure to the drug AZT increased mtDNA copy number in the hearts of female mice [141]. A study of mitochondria that avoid autophagy and effects on cardiac function showed that the hearts of mice that were able to prevent the destruction of mitochondria had no baseline dysfunction, but after TAC showed significantly worsened survival and cardiac hypertrophy [142]. Studies into mitochondrial biogenesis have demonstrated that exposure to endogenous CO can cause increased mitochondrial load in the heart [143], though if this were the driving force, we would expect to see a similar increase in the NCMs. Mitochondrial biogenesis is upregulated after DNA damage [144, 145], potentially through activation of AMPK signaling [146]. Our finding of downregulation of AMPK signaling in the NCMs (Table 3.2) may explain why the NCMs did not demonstrate differential mitochondrial load, and determining whether this is maintained or reversed during cardiac growth could reveal the mechanism of action behind the observed increased mitochondrial load. The presence of increased mitochondria may also lead to increase ROS production [147], which could compound the effect of TAC in our model.

Though we have studied the transcriptome of adult hearts exposed *in utero* to DE and discovered significantly altered transcripts, understanding the transcriptional changes in the adult cardiomyocytes seems to be critical in determining the effect of *in utero* DE exposure on the function of cardiomyocytes both at baseline and in pressure-overload induced heart failure. By both obtaining RNA-seq data from isolated cardiomyocytes and respiratory capabilities of the hearts from *in utero* exposed TAC mice, we could clarify the potential role of metabolic dysregulation in our model of exposure-related heart failure. Overall, our findings of transcriptional dysregulation in NCMs as a result of *in utero* DE exposure will aid in guiding the experimental focus for determining modifications in cardiac function caused by exposure.

Figure 3.1.

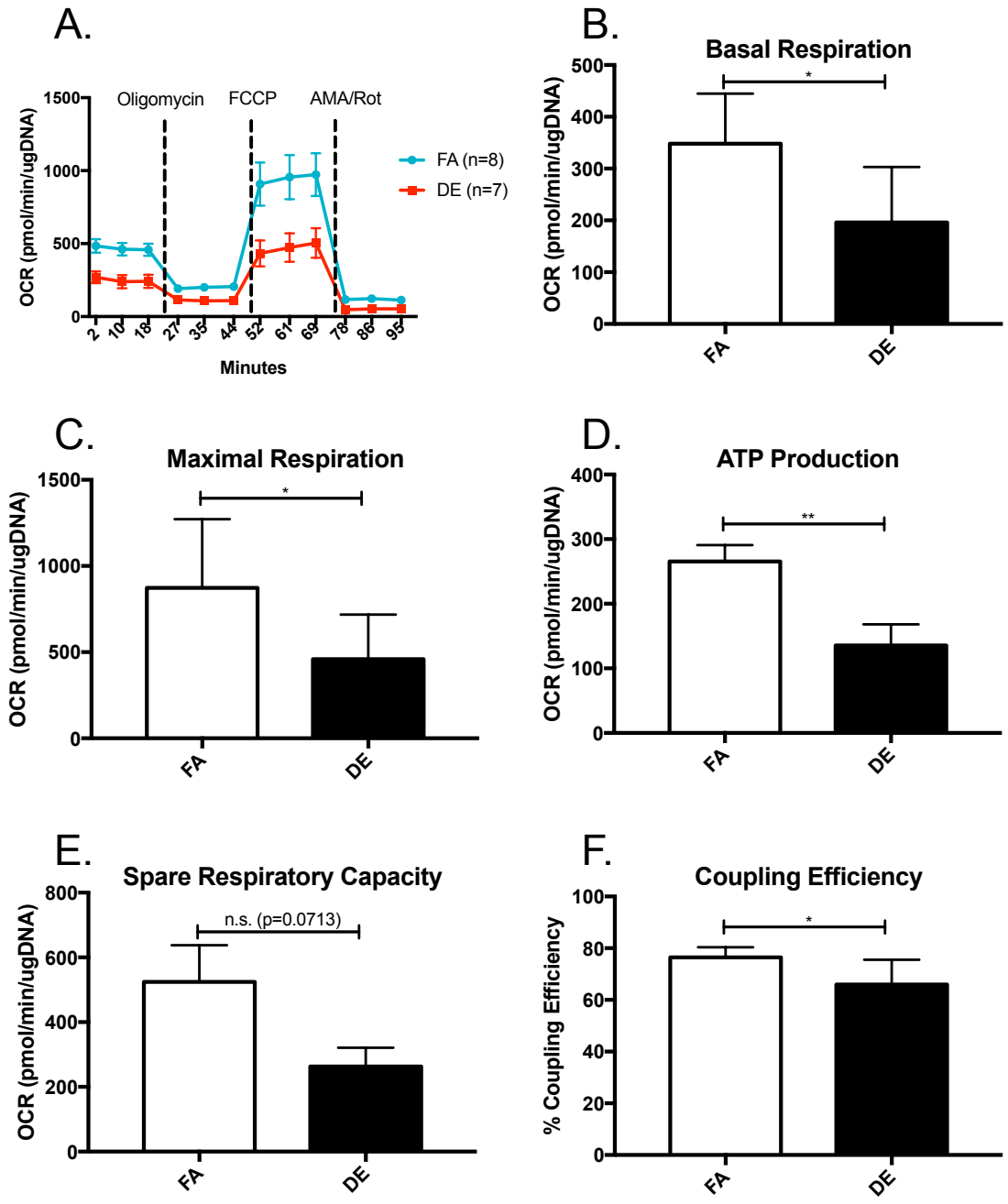

Baseline and maximal oxygen consumption rates are lower in DE NCMs. A. shows the injection scheme and average oxygen consumption rate after injections for all FA and DE NCMs, normalized to total µg DNA. B-F shows

measurements for basal and maximal respiration, ATP production, spare respiratory capacity and coupling efficiency. * indicates p-value <0.05, ** <0.01.

Figure 3.2.

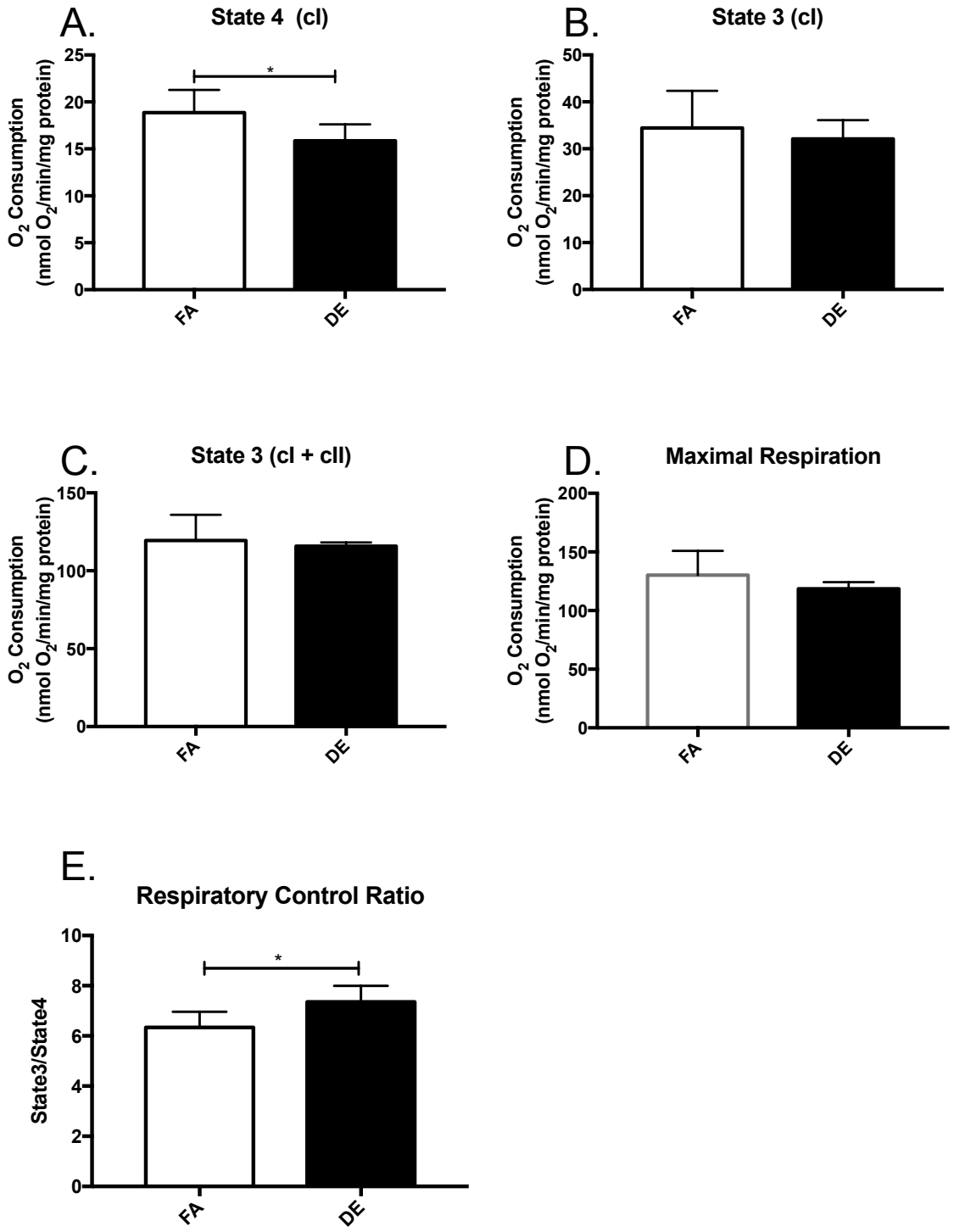

Oxygen consumption rates in isolated mitochondria from adult hearts show increased efficiency when fueled by pyruvate/glutamate. A shows state 4

respiration, B,C shows state 3 respiration drive by cI and cI+II, respectively, D shows maximal respiration, and E shows respiration control ratio (RCR), or the proportion of state 3_{cI}/state 4 respiration. * indicates p-value <0.05.

Figure 3.3.

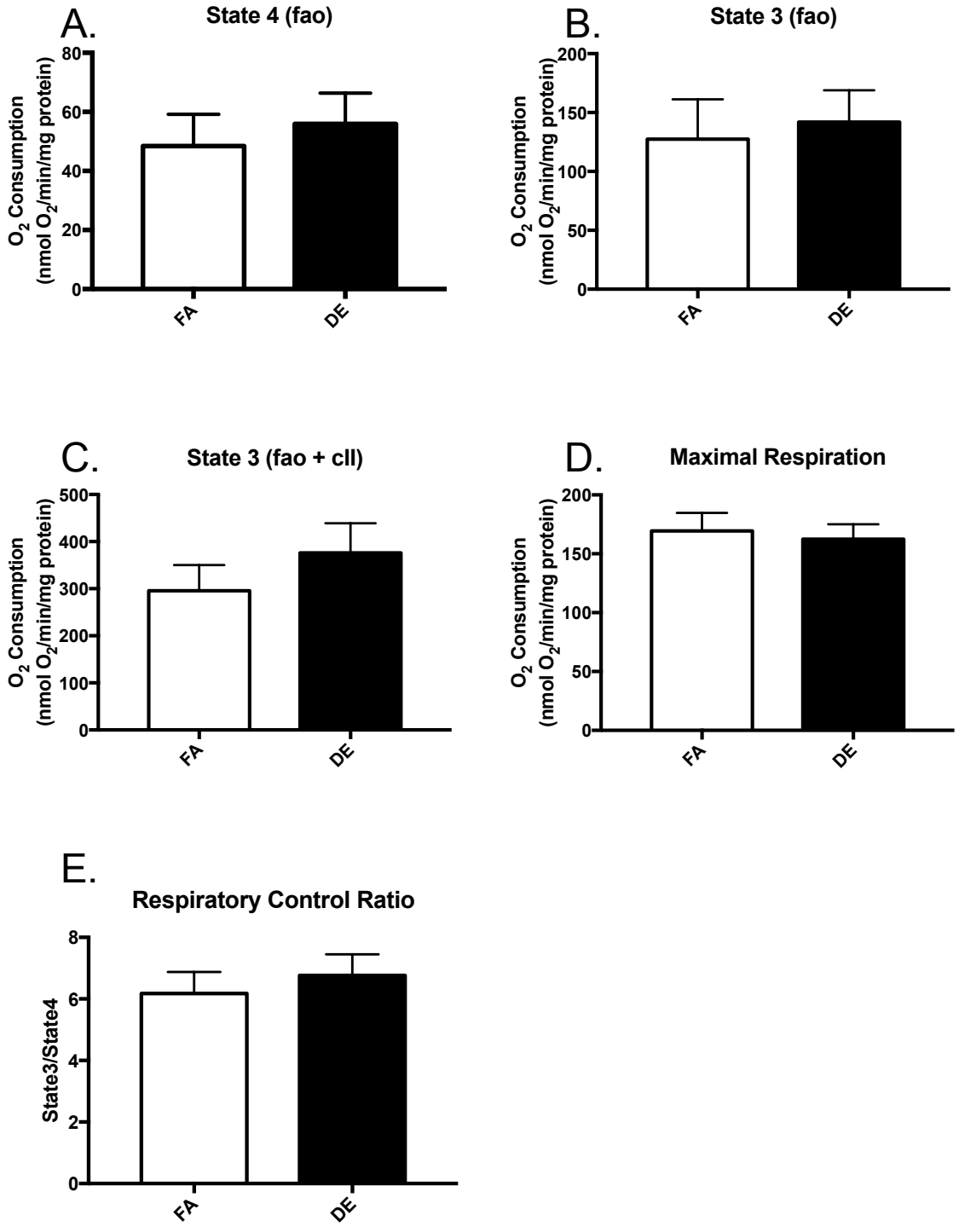

Oxygen consumption rates in isolated mitochondria from adult hearts show similar efficiency when fueled by palmitoyl-L-carnitine. A shows state 4

respiration, B,C shows state 3 respiration drive by fao and fao+cII, respectively, D shows maximal respiration, and E shows RCR, or the proportion of state 3_{fao}/state 4 respiration.

Figure 3.4.

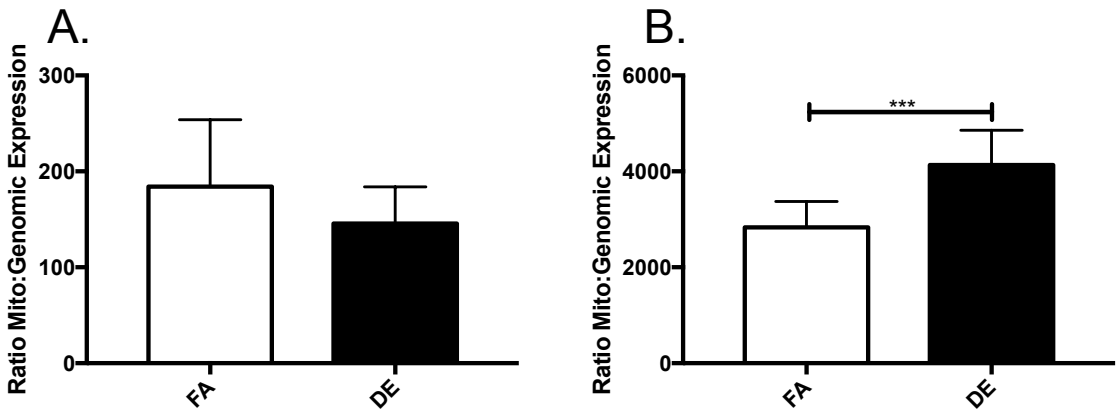

mtDNA copy number as measured by the ratio of mitochondrial expression of mMito to genomic expression of mB2M in A. isolated neonatal cardiomyocytes and B. adult heart tissue. *** indicates p-value <0.001.

Table 3.1. Top ten specific genes showing differential expression due to *in utero* DE exposure

Gene Symbol	**Gene Name**	**Log fold change**	**FDR**
Acot1	acyl-CoA thioesterase 1	-2.25	2.30E-50
Slc25a34	solute carrier family 25, member 34	-3.32	1.34E-39
Acot2	acyl-CoA thioesterase 2	-1.80	4.11E-36
Scd4	stearoyl-coenzyme A desaturase 4	-2.67	5.93E-34
Tfrc	transferrin receptor	-1.70	8.60E-21
Hsdl2	hydroxysteroid dehydrogenase like 2	-1.37	6.50E-19
Hmgcs2	3-hydroxy-3-methylglutaryl-Coenzyme A synthase 2	-4.98	1.34E-18
Cpt1a	carnitine palmitoyltransferase 1a, liver	-1.49	6.29E-17
Angptl4	angiopoietin-like 4	-2.06	7.27E-15
Mlycd	malonyl-CoA decarboxylase	-1.24	7.00E-12

Table 3.2. Top ten pathways showing significantly altered transcription as identified by Ingenuity Pathway Analysis (Qiagen). Arrows indicate expression in DE samples compared to FA.

Ingenuity Canonical Pathway	**p-value**	**Molecules**
Mitochondrial L-carnitine Shuttle Pathway	2.14E-06	↓SLC27A1, ACSL1, CPT1A, CPT2, CPT1B
Fatty Acid β-oxidation	3.47E-06	↓SLC27A1, ACAA2, ACSL1, HADHA, ECI2, HADHB
AMPK Signaling	4.68E-06	↓MLYCD, ADRA1B, PIK3R3, CPT1A, ACACB, LIPE, CPT2, CPT1B ↑ADRA2A, CCND1, PFKL, SLC2A1
Cell Cycle Control of Chromosomal Replication	2.51E-05	↑CDC45, MCM2, MCM3, MCM6, MCM5
LPS/IL-1 Mediated Inhibition of RXR Function	4.17E-05	↓SLC27A1, HMGCS2, ALDH9A1, ACSL1, PPARGC1B, FABP3, CAT, CPT1A, CPT2, CPT1B ↑CHST12, FABP5
GADD45 Signaling	1.00E-04	↑CCNE1, CCND1, PCNA, CDK1
Hepatic Fibrosis / Hepatic Stellate Cell Activation	1.70E-04	↑A2M, IGFBP4, PGF, COL27A1, COL5A3, IGFBP3, COL1A1, CCL21 ↓FGF1, MYH6
Ketogenesis	2.57E-04	↓HMGCS2, HADHA, HADHB
Estrogen-mediated S-phase Entry	2.57E-04	↑CCNE1, CCND1, E2F1, CDK1
Oleate Biosynthesis II (Animals)	5.89E-04	↓SCD4 ↑FADS1

Chapter 4

In utero exposure to diesel exhaust particulates modifies DNA methylation in neonatal cardiomyocytes

4.1 INTRODUCTION

Epidemiological studies have demonstrated that exposure to particulate matter air pollution is harmful to cardiovascular health [6, 7, 69]. There is growing evidence of alterations in epigenetic control due to $PM_{2.5}$ exposure. $PM_{2.5}$ and PM_{10} exposure have been correlated with significantly decreased global DNA methylation in blood as indicated by LINE1 and Alu methylation [62, 63, 148], as well as changes in targeted loci such as decreased methylation in the iNOS promoter [63] and increased methylation at the p16 promoter [149]. Diesel exhaust exposure specifically has also been shown to cause dysregulation of epigenetic signatures. Human bronchial epithelial cells exposed to diesel particulates via culture showed dysregulation of >60% of microRNAs [150], and BALB/c mice exposed to diesel exhaust and given allergenic stimuli showed hypermethylation of the interferon-gamma promoter and hypomethylation of interleukin-4 in T-cells [151]. We have also previously shown hypomethylation in exon 1 of GM6307 in NCMs resulting from *in utero* exposure to DE (Chapter 2)[119].

We have performed reduced representation bisulfite sequencing (RRBS) on neonatal cardiomyocytes isolated from pups exposed to either FA or DE *in utero*, and have found diminished methylation at CpG regions in DE NCMs. This

study is the first of its kind to show a widespread cardiomyocyte change in DNA methylation as a result of *in utero* exposure.

4.2 METHODS

Reduced representation bisulfite sequencing

NCMs were isolated following the protocol detailed in Chapter 2.2 and frozen. DNA was isolated from frozen p0 isolated cardiomyocytes using Qiagen (Germantown; MD, USA) DNeasy Blood and Tissue kit, according to the manufacturer's protocol. 500 ng of DNA were digested overnight with MspI (New England BioLabs Inc., Ipswich, MA, USA) and then directly prepared with the KAPA Hyper Library prep protocol (KAPA Biosystems, Wilmington, MA, USA). Samples were then adapter-ligated using SeqCap Adapters (Roche-Nimblegen, Pleasanton, CA, USA), and cleaned using a 2.5X post-ligation Agencourt AMPure XP bead cleanup (Beckman Coulter, Indianapolis, IN). Size selection was performed to a size range of 160bp-340bp on a 2% Pippin Prep gel (Sage Science, Beverly, MA, USA), followed by bisulfite conversion using the Zymo EZ DNA Methylation Lightning kit (Zymo Research, Irvine, CA, USA). The converted DNA was then put back into the KAPA Hyper Library prep protocol at the library amplification step, and amplification was performed with 19 PCR cycles using 2X KAPA Hifi HotStart Uracil+ ReadyMix (KAPA Biosystems, Wilmington, MA, USA). Post-amplification cleanup was performed with 0.8X Agencourt AMPure XP beads (Beckman Coulter). Library size distributions were validated using the

Agilent High Sensitivity D1000 ScreenTape run on an Agilent 2200 TapeStation (Agilent Technologies, Inc., Santa Clara, CA, USA). Additional library QC, blending of pooled indexed libraries, and cluster optimization was performed using Life Technologies- Invitrogen Qubit® 2.0 Fluorometer (Life Technologies-Invitrogen, Carlsbad, CA, USA). Sample libraries were sequenced on the Illumina HiSeq 2500 (Illumina; San Diego, CA, USA).

Sequences were processed by discarding the low quality reads using Illumina's base call quality filter, and raw reads were trimmed of adapter sequences and flanking low quality base reads using the trimmomatic read trimmer [79], discarding any reads less than 25nt. Reads were aligned to the mm10 genomes using the Bismark aligner [80], read using the Bioconductor bsseq package [82], and differential methylation was called using the Bioconductor DSS package [83]. To be considered a differentially methylated region (DMR), a) sequences had to have read coverage >5 in at least half of the samples, b) the region had to be at least 50bp in length with at least 3 CpGs present, and c) at least 50% of the CpGs in the region had to be significant, based on a $p < 0.001$ and show a minimum 10% difference in methylation. Any significant DMRs within 100bp of each other were merged to a single DMR. DMRs were given estimate gene calls based on the closest genes.

4.3 RESULTS

In utero exposure to DE results in altered DNA methylation patterning

The temporal delay between *in utero* exposure, changes in adult gene expression (Chapter 2)[119] and adult onset of disease [16] suggests that an epigenetic mechanism may mediate the observed effects on adult increased susceptibility to heart failure. We performed reduced RRBS on isolated NCMs from p0 mice exposed to *in utero* FA or DE to uncover alterations in DNA methylation at potential regions of control. We identified 63 differentially methylated regions (DMRs), of which only 1 was hypermethylated in the DE samples. The top ten DMRs and their gene calls are represented in Table 4.1. To determine whether any particular pathways were being selectively altered in their DNA methylation as a result of exposure, we performed pathway analysis using Qiagen Ingenuity Pathway Analysis (Qiagen). Genes that were called to have DMRs were given a hypothesized significant change of expression, with decreased methylation given a call of increased expression and vice versa. The top ten pathways showing altered DNA methylation are presented in Table 4.2. While this is not a perfect test, as we have no guarantee that the DMRs affect the genes we have called them connected to, nor do we know if transcription would be affected in the manner we have described, the finding of genes involved in pathways such as β-adrenergic, G protein-coupled receptor, and hypertrophic signaling being significantly affected by altered DNA methylation indicates a clear cardiac pattern.

In utero exposure to DE significantly decreases DNA methylation in regulatory regions

The discovery of 62 DMRs showing decreased methylation and only 1 showing an increase in the DE NCMs suggests a significant loss of methylation in the DE NCMs. In fact, in figure 4.1 when we display each CpG sequenced and group by the percentage of times that CpG was found to be methylated in each sample and compare the two groups, we can see a clear decrease in the amount of methylation present in the DE samples, both through a higher proportion of 0-5% methylated CpGs and the lower amount of CpGs that were found to be methylated in >25% of the sequences.

When evaluating the individual CpGs that were identified to have significantly different methylation status between the FA and DE NCMs given an FDR of 0.1, including those that were incorporated into DMRs, we identified 12,629 differentially methylated CpGs (564 of which were included in DMRs). Of those, only 293 showed increased methylation in the DE NCMs. Assuming a null hypothesis of differential methylation affecting the samples equally, under the binomial distribution we would reject the null hypothesis with a p-value of 2.2e-16. Taken together, these indicate that *in utero* exposure to DE significantly decreases DNA methylation in CpG-rich regions.

4.4 DISCUSSION

The link between findings of adult cardiovascular disease and *in utero* exposure suggest some long-lasting mechanism of action. Alterations of

epigenetics through DNA hypomethylation have been implicated in the development and progression of cardiovascular disease [152, 153], and due to the double-stranded nature of CpG methylation these changes are incredibly stable [154]. Changes in DNA methylation both at the targeted level and genome-wide have been associated with exposure to air pollution (Chapter 2)[119, 155]. We are the first to demonstrate a change in DNA methylation at CpG-rich regions of cardiomyocytes as a result of *in utero* exposure to DE. The discovery of decreased methylation in DMRs associated with genes involved in GPCR and cardiac hypertrophic signaling suggests a cardiac-specific phenotype, though there was no observed increase in transcription of *Gnas*, *Gng12*, *Adra2c* or *Pde6h* in the transcriptional profile of DE NCMs (Chapter 3). It is possible that the changes in transcription affected by DNA methylation would be activated through stress, or were expressed embryonically.

It is unclear whether this change in DNA methylation is occurring through a directed or undirected pathway. Passive removal of DNA methylation can occur due to oxidative damage from ROS [109, 156], as discussed in Chapter 2.4. If this process is occurring early in development during the repatterning of methylation, these changes would be extremely heritable, and likely occurring in multiple cell and organ types [154]. Targeted changes in DNA methylation in response to air pollution have been described, for example, a study using a mouse model of $PM_{2.5}$ exposure found that the alveolar epithelial cells of these mice displayed hypermethylation of the p16 promoter alongside increased DNMT1 expression [149], and our finding of decreased methylation on the first

exon of GM6307 as a result of *in utero* DE exposure (Chapter 2)[119]. Our prior findings of transcriptional dysregulation in NCMs did not identify any DNA methyltransferase genes as being differentially expressed (Chapter 3), though the original change may have occurred earlier in development and maintained till birth. Interestingly, we did find significantly increased expression of *Mthfd2* and *Mthfd1L* in the DE NCMs, which would suggest an increased availability of methionine to enter the S-adenosyl methionine cycle and produce methyl groups [157]. Assessing DNMT expression in the heart at multiple embryonic developmental stages would help clarify the mechanism behind the observed loss of methylation.

Figure 4.1

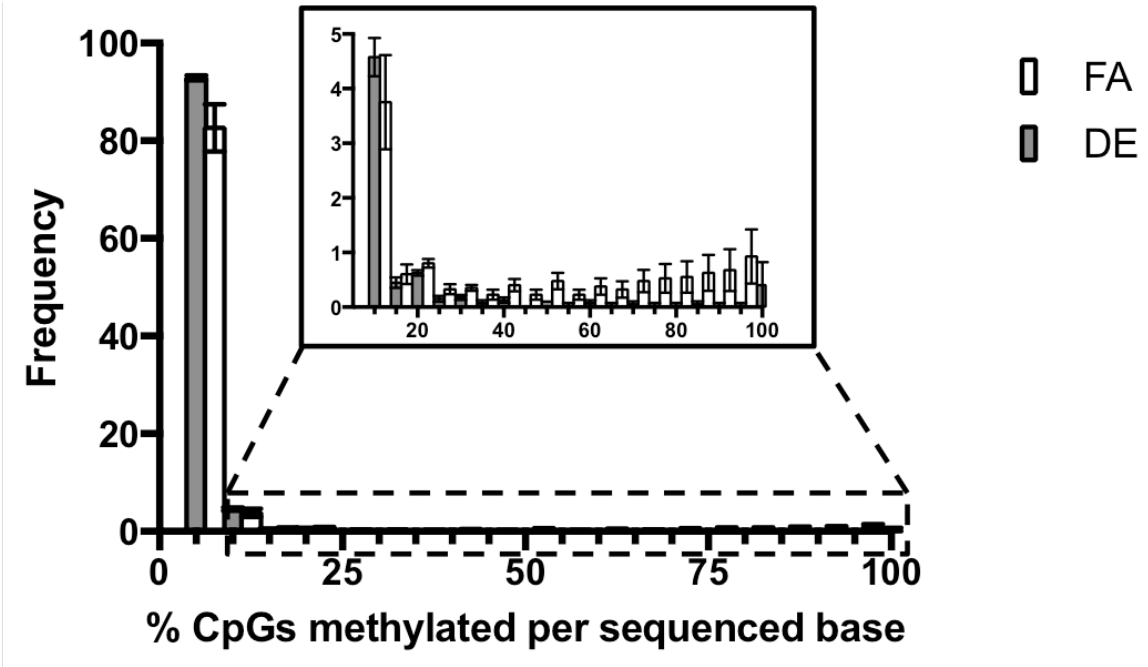

Histogram of % sequences methylated within sequenced CpGs. Individual CpGs were analyzed and placed into 5% incremental bins displaying the % of sequences methylated.

Table 4.1 Top ten significant DMRs in NCMs associated with *in utero* DE exposure.

Gene	Chromosome	Start	End	# CpGs	AreaStat
3110070M22Rik	chr13	119488228	119488562	90	-1875.261
Grb10	chr11	12026282	12026469	49	-715.823
1700030C10Rik	chr12	20232946	20234272	36	-465.281
Mid1	chrX	169994141	169994213	16	-332.462
Zfp444	chr7	6189544	6189675	24	-218.944
Erdr1	chrY	90807240	90807512	13	-214.273
Unc45b	chr11	82933209	82933329	22	-195.998
Gm13152	chr4	147219459	147219685	17	-138.560
H13	chr2	152686786	152687008	13	-118.630
Gnas	chr2	174297352	174297431	10	-95.560

Table 4.2 Top ten pathways with altered DNA methylation. All molecules listed have shown decreased methylation in the associated DMRs.

Ingenuity Canonical Pathway	p-value	Molecules
Cardiac Hypertrophy Signaling	0.002	MAP3K9, GNAS, ADRA2C, GNG12
$G_{\alpha s}$ Signaling	0.002	RAPGEF2, GNAS, GNG12
G Protein Signaling Mediated by Tubby	0.003	GNAS, GNG12
$G_{\alpha i}$ Signaling	0.003	GNAS, ADRA2C, GNG12
Cardiac β-adrenergic Signaling	0.004	GNAS, GNG12, PDE6H
Relaxin Signaling	0.004	GNAS, GNG12, PDE6H
Ephrin Receptor Signaling	0.008	EPHA7, GNAS, GNG12
CCR5 Signaling in Macrophages	0.012	GNAS, GNG12
Ephrin B Signaling	0.013	GNAS, GNG12
Protein Kinase A Signaling	0.014	PTPRU, GNAS, GNG12, PDE6H

Chapter 5

Conclusions and Future Directions

We have described not only the transcriptional dysregulation that occurs in neonatal cardiomyocytes and adult heart tissue as a response to *in utero* exposure and adult TAC surgery, but also the changes in DNA methylation as a result of exposure, both at targeted loci and in global regulatory regions. From these findings, we have discovered that the metabolic capacity of NCMs is significantly decreased at baseline and maximal respiration, indicating a potential defect in oxidative phosphorylation. Conversely, we have also found that the mitochondria of adult hearts have an apparent increase in their respiration capability as measured by the respiratory control ratio, either due to a reversal of the neonatal phenotype, or due to lack of cellular context that affects the metabolic phenotype. Additionally, the adult heart tissue has a higher mitochondrial load, as measured by mtDNA copy number. In sequencing the NCM transcriptome, we have identified dysregulation in metabolic and cell replication pathways. The time points and conditions of sample collection and the tests performed are represented in Figure 5.1. These studies have generated datasets that will lay the groundwork for generating testable hypotheses into the mechanism(s) by which *in utero* DE exposure increases the risk of adult heart failure for both our studies and future investigators.

Understanding the maternal contribution to our model of exposure-driven adult susceptibility to heart failure can give valuable insight into the driving forces

of dysfunction within the heart. Nutritional and pharmacological intervention studies can be used to determine the influence of maternal immune activation and ROS generation as a result of exposure. Treating pregnant dams during exposure with anti-inflammatory drugs such as low-dose NSAIDs, as well as directly inhibiting cytokines such as IL-6 or TNFα through siRNA treatment or decreasing their expression using transgenic models, and examining adult offspring susceptibility to heart failure in our TAC model would reveal the importance of the maternal inflammatory reaction in fetal cardiovascular remodeling.

To tease apart the influence of ROS on both the adult phenotype and cardiomyocyte DNA methylation, pregnant dams could be given antioxidants such as *N*-acetylcysteine [158] or vitamin E [159, 160], and the NCMs examined for DNA methylation status. Furthermore, if the NCMs do revert to a similar DNA methylation status when compared to FA controls, then using these mice in our TAC model would allow us to examine the role of DNA hypomethylation as a contributor to increased adult susceptibility to heart failure. Similarly, increasing maternal dietary nutrients that feed into the S-adenosyl methionine pathway such as vitamin B_6 or B_{12} and testing the offspring outcome in our model can clarify whether the decreased DNA methylation is a result of lack of methyl donors. Dietary B_6 and B_{12} have improved patient outcome in regards to $PM_{2.5}$ mediated increase of heart rate variability [161], and we observed an increase in expression of *Mthfd2* and *1L* in the NCMs of *in utero* DE-exposed mice. It is possible that metabolic pathways, such as the transsulfuration pathway that

converts homocysteine to cystathionine for later glutathione generation, are depleting methyl-donors, which can lead to hypomethylation of DNA [162, 163].

We would also like to know if the NCMs themselves have increased ROS activity, or if the placental environment is the main contributor. Probing placentas and NCMs from *in utero* DE exposed mice for 8-oxoguanine, one of the most common oxidative DNA lesions [164], will not only reveal differential intracellular ROS activity, but if it were present in the NCMs, could give an indication of whether ROS is playing a role in the hypomethylated status of these cells. Alongside this, measuring DNMT1 and DNMT3a/b expression during embryonic development can reveal whether the lack of methylation is due to decreased methyltransferase transcription, or DNA damage and failure to reestablish methylation.

While understanding the changes in transcription that accompany *in utero* exposure in NCMs is informative of early cellular changes, it would be informative to discover which transcripts are showing dysregulation in the adult cardiomyocytes after TAC. As discussed in Chapter 2, the reason we may have identified so few altered transcripts in the adult heart may be due to interfering signal from the various cell-types present. Performing RNA-seq in the isolated adult cardiomyocytes would allow for an unobstructed view of transcriptional changes associated with *in utero* DE exposure and adult TAC surgery. Similarly, while our finding of decreased methylation at regulatory regions within NCMs is the first of its kind, there are changes in the methylome associated with cardiomyocyte maturation [106]. By performing RRBS on isolated adult

cardiomyocytes from *in utero* DE exposed mice after TAC surgery, we would be able to determine 1) if the decreased methylation observed in the neonatal stage is maintained through adult development, and 2) if the adult TAC model of pressure overload hypertrophy has exacerbating effects on the adult cardiomyocyte methylome.

Finally, our discovery of impaired pyruvate/glutamate-fueled cellular respiration in the NCMs of *in utero* DE exposed mice and the apparent reversal of the phenotype in adult needs further study. To determine the impact of cellular context on the observed respiration rates, we need to repeat the study using mitochondria isolated from NCMs to determine whether the previously observed decreased oxygen consumption at baseline and maximal respiration, as well as decreased coupling efficiency, are consistent despite cellular context or require the cellular environment to detect these effects. Likewise, by testing the respiratory capability of homogenized adult cardiac tissue, we can determine whether the presence of cellular context maintains the observed increase in RCR in DE mice. This may also allow for any potential differences in respiration due to fatty acid oxidation to be measureable.

Figure 5.1

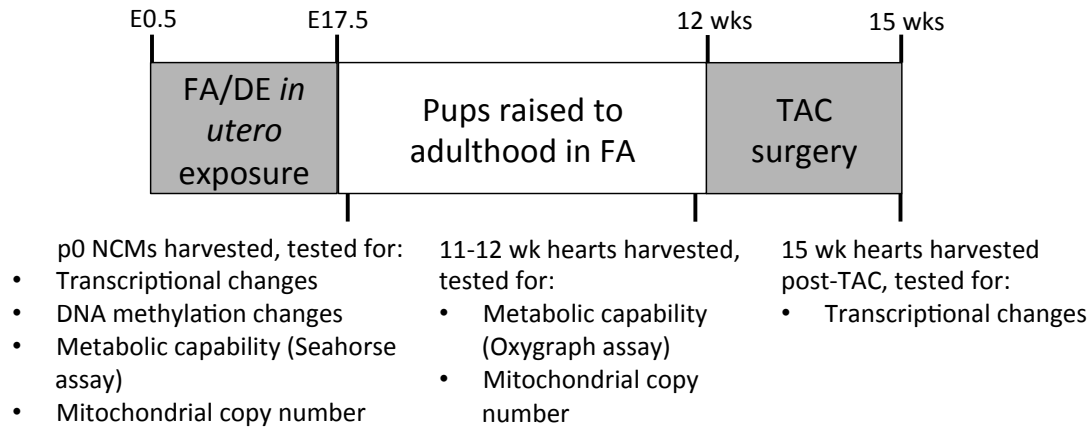

A summary of the time points and conditions of the experiments described in this dissertation.

References

1. Ling S, van Eeden SF. (2009) Particulate matter air pollution exposure: role in the development and exacerbation of chronic obstructive pulmonary disease. *International Journal of Chronic Obstructive Pulmonary Disease*. 4:233-243.
2. Ni L, Chuang C, Zuo L. (2015) Fine particulate matter in acute exacerbation of COPD. *Front Physiol*. 6:294.
3. Pope Cr, Burnett RT, Thun MJ, Calle EE, Krewski D, Ito K, Thurston GD. (2002) Lung cancer, cardiopulmonary mortality, and long-term exposure to fine particulate air pollution. *JAMA*. 287(9):1132-41.
4. Wang Y, Eliot MN, Wellenius GA. (2014) Short-term changes in ambient particulate matter and risk of stroke: A systematic review and meta-analysis. *J Am Heart Assoc*. 3(4):e000983.
5. Zhang P, Dong G, Sun B, Zhang L, Chen X, Ma N, Yu F, Guo H, Huang H, Lee YL, Tang N, Chen J. (2011) Long-term exposure to ambient air pollution and mortality due to cardiovascular disease and cerebrovascular disease in Shenyang, China. *PLoS One*. 6(6):e20827.
6. Brook R, Rajagopalan S, Pope CA 3rd, Brook JR, Bhatnagar A, Diez-Roux AV, et al. (2010) Particulate matter air pollution and cardiovascular disease: An update to the scientific statement from the American Heart Association. *Circulation*. 121(21):2331-78.
7. Bhatnagar A. (2006) Environmental cardiology: studying mechanistic links between pollution and heart disease. *Circulation Research*. 99:692-705.
8. Milojevic A, Wilkinson P, Armstrong B, Bhaskaran K, Smeeth L, Hajat S. (2014) Short-term effects of air pollution on a range of cardiovascular events in England and Wales: case-crossover analysis of the MINAP database, hospital admissions and mortality. *Heart*. 100:1093-1098.
9. de Kok T, Driece HA, Hogervorst JG, Briedé JJ. (2006) Toxicological assessment of ambient and traffic-related particular matter: a review of recent studies. *Mutat Res*. 613(2-3):103-122.
10. Barker D, Osmond C. (1986) Infany mortality, childhood nutrition, and ischaemic heart disease in England and Wales. *Lancet*. 1(8489):1077-1081.
11. Barker D, Osmond C, Golding J, Kuh D, Wadsworth ME. (1989) Growth in utero, blood pressure in childhood and adult life, and mortality from cardiovascular disease. *BMJ (Clinical Research Ed)*. 298(6673):564-7.
12. van den Hooven E, Pierik FH, de Kluizenaar Y, Hofman A, van Ratingen SW. (2012) Air pollution exposure and markers of placental growth and function: the Generation R Study. *Environ Health Perspect*. 120(12):1753-1759.
13. Yorifuji T, Naruse H, Kashima S, Murakoshi T, Tsuda T, et al. (2012) Residential proximity to major roads and placental/birth weight ratio. *Sci Total Environ*. 414:98-102.
14. Salafia C, Charles AK, Maas EM. (2006) Placenta and fetal growth restriction. *Clin Obstet Gynecol*. 49(2):236-256.

15. Valentino S, Tarrade A, Aioun J, Mourier E, Richard C, et al. (2016) Maternal exposure to diluted diesel engine exhast alters placental function and induces intergenerational effects in rabbits. *Part Fibre Toxicol*. 13:39.
16. Weldy C, Liu Y, Liggitt HD, Chin MT. (2014) In utero exposure to diesel exhaust air pollution promotes adverse intrauterine conditions, resulting in weight gain, altered blood pressure, and increased susceptibility to heart failure in adult mice. *PLoS One*. 9(2):e88582.
17. Rocha E Silva I, Lichtenfels AJ, Amador Pereira LA, Saldiva PH. (2008) Effects of ambient levels of air pollution generated by traffic on birth and placental weights in mice. *Fertil Steril*. 90(5):1921-1924.
18. Fujimoto A, Tsukue N, Watanabe M, Sugawara I, Yanagisawa R, et al. (2005) Diesel exhaust affects immunological action in the placentas of mice. *Environ Toxicol*. 20(4):431-440.
19. Chen J, Schwartz J. (2008) Metabolic syndrome and inflammatory responses to long-term particulate air pollutants. *Environ Health Perspect*. 116(5):612-617.
20. Viehmann A, Hertel S, Fuks K, Eisele L, Moebus S, et al. (2015) Long-term residential exposure to urban air pollution, and repeated measures of systemic blood markers of inflammation and coagulation. *Occup Environ Med*. 72(9):656-663.
21. Peters A, Fröhlich M, Döring A, Immervoll T, Wichmann HE, et al. (2001) Particulate air pollution is associated with an acute phase response in men; results from the MONICA-Augsburg Study. *Eur Heart J*. 22(14):1198-1204.
22. Urch B, Speck M, Corey P, Wasserstein D, Manno M, et al. (2010) Concentrated ambient fine particles and not ozone induce a systemic interleukin-6 response in humans. *Inhal Toxicol*. 22(3):210-218.
23. Tsai D, Amyai N, Marques-Vidal P, Wang JL, Riediker M. (2012) Effects of particulate matter on inflammatory markers in the general adult population. *Part Fibre Toxicol*. 9:24.
24. Romero R, Espinoza J, Gonçalves LF, Kusanovic JP, Friel L, et al. (2007) The role of inflammation and infection in preterm birth. *Semin Reprod Med*. 25(1):21-39.
25. Boyle A, Rinaldi SF, Norman JE, Stock SJ. (2017) Preterm birth: Inflammation, fetal injury and treatment strategies. *J Reprod Immunol*. 119:62-66.
26. Borzychowski A, Sargent IL, Redman CW. (2006) Inflammation and pre-eclampsia. *Semin Fetal Neonatal Med*. 11(5):309-316.
27. Lee P, Talbott EO, Roberts JM, Catov JM, Sharma RK. (2011) Particulate air pollution exposure and C-reactive protein during early pregnancy. *Epidemiology*. 22(4):524-531.
28. van den Hooven E, de Kluizenaar Y, Pierik FH, Hofman A, van Ratingen SW, et al. (2012) Chronic air pollution exposure during pregnancy and maternal and fetal C-reactive protein levels: the Generation R Study. *Environ Health Perspect*. 120(5):746-751.
29. Saenen N, Vriiens K, Janssen BG, Madhloum N, Peusens M, Gvselaers W, et al. (2016) Placental nitrosative stress and exposure to ambient air pollution during gestation: a population study. *Am J Epidemiol*. 184(6):442-9.

30. Janssen B, Munters E, Pieters N, Smeets K, Cox B, Cuypers A, Fierens F, Penders J, Vangronsveld J, Gyselaers W, Nawrot TS. (2012) Placental mitochondrial DNA contect and particulate air pollution during *in utero* life. *Environmental Health Perspectives*. 120(9):1346-1352.
31. Clemente D, Casas M, Vilahur N, Begiristain H, Bustamante M, et al. (2016) Prenatal ambient air pollution, placental mitochondrial DNA content, and birth weight in the INMA (Spain) and ENVIR*ON*AGE (Belgium) birth cohorts. *Environ Health Perspect*. 124(5):659-665.
32. Clemente D, Casas M, Janssen BG, Lertxundi A, Santa-Marina L, et al. (2017) Prenatal ambient air pollution exposure, infant growth and plaental mitochondrial DNA content in the INMA birth cohort. *Environ Res*. 157:96-102.
33. Bernstein I, Horbar JD, Badget GJ, Ohlsson A, Golan A. (2000) Morbidity and mortality among very-low-birth-weight neonates with intrauterine growth restriction. *Am J Obstet Gynecol*. 182(1):198-206.
34. Sˇ rám R, Binková B, Dejmek J, Bobak M. (2005) Ambient air pollution and pregnancy outcomes: a review of the literature. *Environ Health Perspect*. 113(4):375-382.
35. Stieb D, Chen L, Eshoul M, Judek S. (2012) Ambient air pollution, birth weight and preterm birth: A systemic review and meta-analysis. *Environ Res*. 117:100-111.
36. Shah P, Balkhair T. (2011) Air pollution and birth outcomes: a systemic review. *Environ Int*. 37:498-516.
37. Demicheva E, Crispi F. (2014) Long-term follow-up of intrauterine growth restriction: cardiovascular disorders. *Fetal Diagn Ther*. 36(2):143-153.
38. Baschat A. (2004) Fetal responses to placental insufficiency: an update. *BJOG*. 111(10):1031-1041.
39. Llop S, Ballester F, Estarlich M, Esplugues A, Rebagliato M, et al. (2010) Preterm birth and exposure to air pollutants during pregnancy. *Environ Res*. 110:778-785.
40. Gehring U, Wijga AH, Fischer P, de Jongste JC, Kerkhof M, et al. (2011) Traffic-related air pollution, preterm birth and term birth weight in the PIAMA birth cohort study. *Environ Res*. 111:125-135.
41. Panasevich S, Håberg SE, Aamodt G, London SJ, Stigum H, et al. (2016) Association between pregnancy exposure to air pollution and birth weight in selected areas of Norway. *Arch Public Health*. 74:26.
42. Dadvand P, Parker J, Bell ML, Bonzini M, Brauer M, Darrow LA, et al. (2013) Maternal exposure to particulate air pollution and term birth weight: a mutli-country evaluation of effect and heterogeneity. *Environmental Health Perspectives*. 121(3):367-373.
43. van den Hooven E, Pierik FH, de Kluizenaar Y, Willemsen SP, Hofman A, van Ratingen SW, et al. (2012) Air pollution exposure during pregnancy, ultrasound measures of fetal growth, and adverse birth outcomes: a prospective cohort study. *Environ Health Perspect*. 120(1):150-6.

44. Malmqvist E, Liew Z, Källén K, Rignell-Hydbom A, Rittner R, et al. (2017) Fetal growth and air pollution - a study on ultrasound and birth measures. *Environ Res*. 152:73-80.
45. van Rossem L, Rifas-Shiman SL, Melly SJ, Kloog I, Luttmann-Gibson H, Zanobetti A, et al. (2015) Prenatal air pollution exposure and newborn blood pressure. *Environ Health Perspect*. 123(4):353-9.
46. Breton C, Yao J, Millstein J, Gao L, Siegmund KD, et al. (2016) Prenatal air pollution exposures, DNA methyl transferase genotypes, and associations with newborn LINE1 and Alu methylation and childhood blood pressure and carotid intima-media thickness in the Children's Health Study. *Environ Health Perspect*. 124(12):1905-1912.
47. Chen X, Wang Y. (2008) Tracking of blood pressure from childhood to adulthood: a systemic review and meta-regression analysis. *Circulation*. 117(25):3171-3180.
48. Dolk H, Armstrong B, Lachowycz K, Vrijheid M, Rankin J, et al. (2010) Ambient air pollution and risk of congenital anomalies in England, 1991-1999. *Occup Environ Med*. 67(4):223-227.
49. Gilboa S, Mendola P, Olshan AF, Langlois PH, Savitz DA, et al. (2005) Relation between ambient air quality and selected birth defects, seven county study, Texas, 1997-2000. *Am J Epidemiol*. 162(3):238-252.
50. Zhang B, Liang S, Zhao J, Qian Z, Bassig BA, et al. (2016) Maternal exposure to air pollutant PM2.5 and PM10 during pregnancy and risk of congenital heart defects. *J Expo Sci Environ Epidemiol*. 6(4):422-427.
51. Breton C, Mack WJ, Yao J, Berhane K, Amadeus M, Lurmann F, et al. (2016) Prenatal air pollution exposure and early cardiovascular phenotypes in young adults. *PLoS One*. 11(3):e0150825.
52. Weldy C, Liu Y, Chang YC, Medvedev IO, Fox JR, Larson TV, et al. (2013) *In utero* and early life exposure to diesel exhaust air pollution increases adult susceptibility to heart failure in mice. *Part Fibre Toxicol*. 10(1):59.
53. Tanwar V, Gorr MW, Velten M, Eichenseer CM, Long VP, et al. (2017) In utero particulate matter exposure produces heart failure, electrical remodeling, and epigenetic changes at adulthood. *JAHA*. 6(4):e005796.
54. Gorr M, Velten M, Nelin TD, Youtz DJ, Sun Q, et al. (2014) Early life exposure to air pollution induces adult cardiac dysfunction. *Am J Physiol Heart Circ Physiol*. 307(9):H1353-H1360.
55. Laumbach R, Kipen HM. (2012) Respiratory health effects of air pollution: update on biomass smoke and traffic pollution. *J Allergy Clin Immunol*. 129(1):3-11.
56. Jacquemin B, Siroux V, Sanchez M, Carsin AE, Schikowski T, et al. (2015) Ambient air pollution and adult asthma incidence in six European cohorts (ESCAPE). *Environ Health Perspect*. 123(6):613-621.
57. Bakhireva L, Schatz M, Chambers CD. (2007) Effect of maternal asthma and gestational asthma therapy on fetal growth. *J Asthma*. 44(2):71-76.
58. Mestan K, Yu Y, Matoba N, Cerda S, Demmin B, et al. (2010) Placental inflammatory response is associated with poor neonatal growth: preterm birth cohort study. *Pediatrics*. 125(4):e891-898.

59. Jauniaux E, Poston L, Burton GJ. (2006) Placental-related diseases of pregnancy: involvement of oxidative stress and implications in human evolution. *Hum Reprod Update*. 12(6):747-755.
60. Ott M, Gogvadza V, Orrenius S, Zhivotovsky B. (2007) Mitochondria, oxidative stress and cell death. *Apoptosis*. 12(5):913-922.
61. Grevendonk L, Janssen BG, Vanpoucke C, Lefebvre W, Hoxha M, et al. (2016) Mitochondrial oxidative DNA damage and exposure to particulate air pollution in mother-newborn pairs. *Environ Health*.10.
62. Baccarelli A, Wright RO, Bollati V, Tarantini L, Litonjua AA, Suh HH, et al. (2009) Rapid DNA methylation changes after exposure to traffic particles. *Am J Respir Crit Care Med*. 179(7):572-8.
63. Tarantini L, Bonzini M, Apostoli P, Pegoraro V, Bollati V, Marinelli B, et al. (2008) Effects of particulate matter on genomic DNA methylation content and iNOS promoter methylation. *Environ Health Perspect*. 117(2):217-22.
64. Yauk C, Polyzos A, Rowan-Carroll A, Somers CM, Godschalk RW, Van Schooten FJ, Berndt ML, Pogribny IP, Koturbash I, Williams A, Douglas GR, Kovalchuk O. (2008) Germ-line mutations, DNA damage, and global hypermethylation in mice exposed to particulate air pollution in an urban/industrial location. *PNAS*. 105(2):605-610.
65. Burris H, Rifas-Shiman SL, Baccarelli A, Tarantini L, Boeke C, et al. (2012) Associations of LINE-1 DNA methylation with preterm birth in a prospective cohort study. *J Dev Orig Health Dis*. 3(3):173-181.
66. Lin V, Baccarelli AA, Burris HH. (2016) Epigenetics - a potential mediator between air pollution and preterm birth. *Environ Epigenet*. 2(1).
67. Franco R, Schoneveld O, Georgakilas AG, Panayiotidis MI. (2008) Oxidative stress, DNA methylation and carcinogenesis. *Cancer Lett*. 266(1):6-11.
68. Krishnan T, Adar SD, Szpiro AA, Jorgensen NW, van Hee VC, Barr RG, et al. (2012) Vascular responses to long- and short-term exposure to fine particulate matter: MESA Air (Multi-Ethnic Study of Atherosclerosis and Air Pollution). *J Am Coll Cardiol*. 60(21):2158-66.
69. Pope Cr, Muhlestein JB, May HT, Renlund DG, Anderson JL, Horne BD. (2006) Ischemic heart disease events triggered by short-term exposure to fine particulate air pollution. *Circulation*. 114(23):2443-8.
70. Janssen B, Godderis L, Pieters N, Poels K, Kiciński M, Cuypers A, et al. (2013) Placental DNA hypomethylation in association with particulate air pollution in early life. *Part Fibre Toxicol*. 10:22.
71. Weldy C, Luttrell IP, White CC, Morgan-Stevenson V, Cox DP, Carosino CM, et al. (2013) Glutathione (GSH) and the GSH synthesis gene Gclm modulate plasma redox and vascular responses to acute diesel exhaust inhalation in mice. *Inhal Toxicol*. 25(8):444-54.
72. Gould T, Larson T, Stewart J, Kaufman JD, Slater D, McEwen N. (2008) A controlled inhalation diesel exhaust exposure facility with dynamic feedback control of PM concentration. *Inhal Toxicol*. 20(1):49-52.
73. Yin F, Lawal A, Ricks J, Fox JR, Larson T, Navab M, et al. (2013) Diesel exhaust induces systemic lipid peroxidation and development of dysfunctional pro-

oxidant and proinflammatory high-density lipoprotein. *Arterioscler Thromb Vasc Biol*. 33(6):1153-61.
74. Liu Y, Chien W, Medvedev IO, Weldy CS, Luchtel DL, Rosenfeld ME, Chin MT. (2013) Inhalation of diesel exhaust does not exacerbate cardiac hypertrophy or heart failure in two mouse models of cardiac hypertrophy. *Part Fibre Toxicol*. 10:49.
75. Liao Y, Smyth GK, Shi W. (2013) The subread aligner: fast, accurate and scalable read mapping by seed-and-vote. *Nucleic Acids Res*. 41(10):e108.
76. Greco S, Fasanaro P, Castelvecchio S, D'Alessandra Y, Arcelli D, Di Donato M, et al. (2012) MicroRNA dysregulation in diabetic ischemic heart failure patients. *Diabetes*. 61(6):1633-41.
77. Liu Y, Yu M, Wu L, Chin MT. (2010) The bHLH transcription factor CHF1/Hey2 regulates susceptibility to apoptosis and heart failure after pressure overload. *Am J Physiol Heart Circ Physiol*. 298(6):H2082-92.
78. Xiang F, Sakata Y, Cui L, Youngblood JM, Nakagami H, Liao JK, et al. (2009) Transcription factor CHF1/Hey2 suppresses cardiac hypertrophy through an inhibitory interaction with GATA4. *Am J Physiol Heart Circ Physiol*. 290(5):H1997-2006.
79. Bolger A, Lohse M, Usadel B. (2014) Trimmomatic: A flexible trimmer for Illumina Sequence Data. *Bioinformatics*. 30(15):2114-20.
80. Krueger F, Andrews SR. (2011) Bismark: a flexible aligner and methylation caller for Bisulfite-Seq applications. *Bioinformatics*. 27(11):1571-2.
81. Langmead B, Trapnell C, Pop M, Salzberg SL. (2009) Ultrafast and memory-efficient alignment of short DNA sequences to the human genome. *Genome Biol*. 10(3):R25.
82. Hansen K, Langmead B, Irizarry RA. (2012) BSmooth: from whole genome bisulfite sequencing reads to differentially methylated regions. *Genome Biol*. 13(10):R83.
83. Feng H, Conneely KN, Wu H. (2014) A Bayesian hierarchical model to detect differentially methylated loci from single nucleotide resolution sequencing data. *Nucleic Acids Res*. 42(8):e69.
84. van den Bosch B, Lindsey PJ, van den Bug CMM, van der Vlies SA, Lips DJ, et al. (2006) Early and transient gene expression changes in pressure overload-induced cardiac hypertrophy in mice. *Genomics*. 88(4):480-488.
85. Carè A, Catalucci D, Felicetti F, Bonci D, Addario A, Gallo P, et al. (2007) MicroRNA-133 controls cardiac hypertrophy. *Nature Medicine*. 13(5):613-618.
86. Matkovich S, Wang W, Tu Y, Eschenbacher WH, Dorn LE, Condorelli G, et al. (2010) MicroRNA-133a protects against myocardial fibrosis and modulates electrical repolarization without affecting hypertrophy in pressure-overloaded adult hearts. *Circ Res*. 106(1):166-75.
87. Brauer M, Freedman G, Frostad J, van Donkelaar A, Martin RV, Dentener F, et al. (2016) Ambient air pollution exposure estimation for the Global Burden of Disease 2013. *Environ Sci Technol*. 50(1):79-88.

88. Lewné M, Plato N, Gustavsson P. (2007) Exposure to particles, elemental carbon and nitrogen dioxide in workers exposed to motor exhaust. *Ann Occup Hyg*. 51(8):693-701.
89. Nakayama Y, Nara N, Kawakita Y, Takeshima Y, Arakawa M, Katoh M, et al. (2004) Cloning of cDNA encoding a regeneration-associated muscle protease whose expression is attenuated in cell lines derived from Duchenne muscular dystrophy patients. *Am J Pathol*. 164(5):1773-82.
90. Sharma P, Mackay AJ, Dejene EA, Ramadan JW, Langefeld CD, Palmer ND, et al. (2015) An islet-targeted genome-wide association scan identifies novel genes implicated in cytokine-mediated islet stress in type 2 diabetes. *Endocrinology*. 156(9):3147-56.
91. Lo P, Tanikawa C, Katagiri T, Nakamura Y, Matsuda K. (2015) Identification of novel epigenetically inactivated gene PAMR1 in breast carcinoma. *Oncol Rep*. 33(1):267-73.
92. Tonks N. (2013) Protein tyrosine phosphatases: From housekeeping enzymes to master-regulators of signal transduction. *FEBS J*. 280(2):346-78.
93. Chagnon M, Uetani N, Tremblay ML. (2004) Functional significance of the LAR receptor protein tyrosine phosphatase family in development and diseases. *Biochem Cell Biol*. 82(6):664-75.
94. Zhang W, Li PM, Oswald MA, Goldstein BJ. (1996) Modulation of insulin signal transduction by eutopic overexpression of the receptor-type protein-tyrosine phosphatase LAR. *Mol Endocrinol*. 10(5):575-84.
95. Zabolotny J, Kim YB, Peroni OD, Kim JK, Pani MA, Boss O, et al. (2001) Overexpression of the LAR (leukocyte antigen-related) protein-tyrosin phosphatase in muscle causes insulin resistance. *PNAS*. 98(9):5187-92.
96. Kulas D, Zhang WR, Goldstein BJ, Furlanetto RW, Mooney RA. (1995) Insulin receptor signaling is augmented by antisense inhibition of the protein tyrosine phosphatase LAR. *J Biol Chem*. 270(6):2435-8.
97. Menzaghi C, Paroni G, De Bonis C, Coco A, Vigna C, Miscio G, et al. (2008) The protein tyrosine phosphatase receptor type F (PTPRF) locus is associated with coronary artery disease in type 2 diabetes. *J Intern Med*. 263(6):653-4.
98. Ahmad F, Goldstein BJ. (1997) Functional association between the insulin receptor and the transmembrane protein-tyrosine phosphatase LAR in intact cells. *J Biol Chem*. 272(1):448-57.
99. Liu N, Bezprozvannaya S, Willams AH, Qi X, Richardson JA, Bassel-Duby R, Olson EN. (2008) MicroRNA-133a regulates cardiomyocyte proliferation and suppresses smooth muscle gene expression in the heart. *Genes Dev*. 22(23):3242-54.
100. Drawnel F, Wachten D, Molkentin JD, Maillet M, Aronsen JM, Swift F, et al. (2012) Mutual antagonism between IP(3)RII and miRNA-133a regulates calcium signals and cardiac hypertrophy. *J Cell Biol*. 199(5):783-98.
101. He B, Xiao J, Ren A, Zhang Y, Zhang H, Chen M, et al. (2011) Role of miR-1 and miR-133a in myocardial ischemic postconditioning. *J Biomed Sci*. 18:22.
102. Liu N, Bezprozvannaya S, Shelton JM, Frisard MI, Hulver MW, McMillan RP, et al. (2011) Mice lacking microRNA 133a develop dynamin 2–dependent centronuclear myopathy. *J Clin Invest*. 121(8):3258-68.

103. Chen W, Leung CM, Pan HW, Hu LY, Li SC, Ho MR, Tsai KW. (2012) Silencing of miR-1-1 and miR-133a-2 cluster expression by DNA hypermethylation in colorectal cancer. *Oncol Rep*. 28(3):1069-76.
104. Huang L, Xi Z, Wang C, Zhang Y, Yang Z, Zhang S, et al. (2016) Phenanthrene exposure induces cardiac hypertrophy via reducing miR-133a expression by DNA methylation. *Sci Rep*. 6:20105.
105. Westerholm R, Christensen A, Törnqvist M, Ehrenberg L, Rannug U, Sjögren M, et al. (2001) Comparison of exhaust emissions from Swedish environmental classi ed diesel fuel (MK1) and European Program on Emissions, Fuels and Engine Technologies (EPEFE) reference fuel: a chemical and biological characterization. *Environ Sci Technol*. 35(9):1748-54.
106. Gilsbach R, Preissl S, Gruning BA, Schnick T, Burger L, et al. (2014) Dynamic DNA methylation orchestrates cardiomyocyte development, maturation and disease. *Nature Communications*. 5:288.
107. Wauters A, Dreyfuss C, Pochet S, Hendrick P, Berkenboom G, van de Borne P, Argacha JF. (2013) Acute exposure to diesel exhaust impairs nitric oxide-mediated endothelial vasomotor function by increasing endothelial oxidative stress. *Hypertension*. 62(2):352-358.
108. Zuo L, Youtz DJ, Wold LE. (2011) Particulate matter exposure exacerbates high glucose-induced cardiomyocyte dysfunction through ROS generation. *PLoS One*. 6(8):e23116.
109. Valinluck V, Tsai H, Rogstad DK, Burdzy A, Bird A, Sowers LC. (2004) Oxidative damage to methyl-CpG sequences inhibits the binding of the methyl-CpG binding domain (MBD) of methyl-CpG binding protein 2 (MeCP2). *Nucleic Acids Res*. 32(14):4100-4108.
110. Hackett J, Sengupta R, Zylicz JJ, Murakami K, Lee C, Down TA, Surani MA. (2013) Germline DNA demethylation dynamics and imprint erasure through 5-hydroxymethylcytosine. *Science*. 339(6118):448-452.
111. Guo J, Su Y, Zhong C, Ming G, Song H. (2011) Hydroxylation of 5-methylcytosine by TET1 promotes active DNA demethylation in the adult brain. *Cell*. 145(3):423-434.
112. Brenet F, Moh M, Funk P, Feierstein E, Viale AJ, Socci ND, Scandura JM. (2011) DNA methylation of the first exon is tightly linked to transcriptional silencing. *PLoS One*. 6(1):e14524.
113. García R, Villar AV, Cobo M, Llano M, Martín-Durán R, Hurlé MA, Nistal JF. (2013) Circulating levels of miR-133a predict the regression potential of left ventricular hypertrophy after valve replacement surgery in patients with aortic stenosis. *J Am Heart Assoc*. 2(4):e000211.
114. Dakhlallah D, Zhang J, Yu L, Marsh CB, Angelos MG, Khan M. (2015) MicroRNA-133a engineered mesenchymal stem cells augment cardiac function and cell survival in the infarct heart. *J Cardiovasc Pharmacol*. 65(3):241-51.
115. To T, Zhu J, Villeneuve PJ, Simatovic J, Feldman L, Gao C, Williams D, Chen J, Weichenthal S, Wall C, Miller AB. (2015) Chronic disease prevalence in women and air pollution--A 30-year longitudinal cohort study. *Environment International*. 80:26-32.

116. Heck J, Wu J, Lombardi C, Qiu J, Meyers TJ, et al. (2013) Childhood cancer and traffic-related air pollution exposure in pregnancy and early life. *Environ Health Perspect*. 121:1385–1391.
117. Eze I, Hemkens LG, Bucher HC, Hoffmann B, Schindler C, et al. (2015) Association between ambient air pollution and diabetes mellitus in Europe and North America: systematic review and meta-analysis. *Environ Health Perspect*. 123(5):381-389.
118. Mitanchez D, Yzydorczyk C, Simeoni U. (2015) What neonatal complications should the pediatrician be aware of in case of maternal gestational diabetes? *World J Diabetes*. 6(5):734-743.
119. Goodson J, Weldy CS, MacDonald JW, Liu Y, Bammler TK, et al. (2017) In utero exposure to diesel exhaust particulates is associated with an altered cardiac transcriptional response to transverse aortic constriction and altered DNA methylation. *FASEB J*.
120. Boehm E, Jones BE, Radda GK, Veech RL, Clarke K, et al. (2001) Increased uncoupling proteins and decreased efficiency in palmitate-perfused hyperthyroid rat heart. *Am J Physiol Heart Circ Physiol*. 280(3):H977-983.
121. Kim D, Pertea G, Trapnell C, Pimentel H, Kelley R, et al. (2013) TopHat2: accurate alignment of transcriptomes in the presence of insertions, deletions and gene fusions. *Genome Biol*. 14:R36.
122. McKenna A, Hanna M, Banks E, Sivanchenko A, Cibulskis K, et al. (2010) The Genome Analysis Toolkit: a MapReduce framework for analyzing next-generation DNA sequencing data. *Genome Res*. 20(9):1297-1303.
123. DePristo M, Banks E, Poplin R, Garimella KV, Maguire JR, et al. (2011) A framework for variation discovery and genotyping using next-generation DNA sequencing data. *Nat Genet*. 43(5):491-498.
124. Trapnell C, Hendrickson DG, Sauvageau M, Goff L, Rinn JL, et al. (2013) Differential analysis of gene regulation at transcript resolution with RNA-seq. *Nat Biotech*. 31:46-53.
125. Malik A, Czajka A, Cunninham P. (2016) Accurate quantification of mouse mitochondrial DNA without co-amplification of nuclear mitochondrial insertion sequences. *Mitochondrion*. 29:59-64.
126. Taegtmeyer H, Sen S, Vela D. (2010) Return to the fetal gene program: a suggested metabolic link to gene expression in the heart. *Ann N Y Acad Sci*. 1188:191-198.
127. Onay-Besikci A, Campbell FM, Hopkins TA, Dyck JR, Lopaschuk GD. (2003) Relative importance of malonyl CoA and carnitine in maturation of fatty acid oxidation in newborn rabbit heart. *Am J Physiol Heart Circ Physiol*. 284(1):H283-289.
128. Brand M, Nicholls DG. (2011) Assessing mitochondrial dysfunction in cells. *Biochem J*. 435(Pt 2):297-312.
129. Ingwall J. (2008) Energy metabolism in heart failure and remodelling. *Cardiovasc Res*. 81(3):412-419.
130. Fürstenwerth H. (2012) Rethinking heart failure. *Cardiol Res*. 3(6):243-257.
131. Stanley W, Recchia FA, Lopaschuk GD. (2005) Myocardial substrate metabolism in the normal and failing heart. *Physiol Rev*. 85(3):1093-1129.

132. Wei Y, Zhang JJ, Li Z, Gow A, Chung KF, et al. (2016) Chronic exposure to air pollution particles increases the risk of obesity and metabolic syndrome: findings from a natural experiment in Beijing. *FASEB J*. 30(6):2115-2122.
133. Rajagopalan S, Brook RD. (2012) Air pollution and type 2 diabetes: mechanistic insights. *Diabetes*. 61(12):3037-3045.
134. Eze I, Schaffner E, Foraster M, Imboden M, von Eckardstein A, et al. (2015) Long-term exposure to ambient air pollution and metabolic syndrome in adults. *PLoS One*. 10(6):e0130337.
135. Divakaruni A, Brand MD. (2011) The regulation and physiology of mitochondrial proton leak. *Physiology*. 26(3):192-205.
136. Anmann T, Guzun R, Beraud N, Pelloux S, Kuznetsov AV, et al. (2006) Different kinetics of the regulation of respiration in permeabilized cardiomyocytes and in HL-1 cardiac cells. Importance of cell structure/organization for respiration regulation. *Biochim Biophys Acta*. 1757(12):1597-1606.
137. Velasco C, Draxi A, Wiethüchter A, Eigentler A, Gnaiger E. (2012-2013) Mitochondrial respiration in permeabilized fibres versus homogenate from trout heart and liver. *Mitochondr Physoil Network*. 1-12.
138. Pisano A, Cerbelli B, Perli E, Pelullo M, Bargelli V, et al. (2016) Impaired mitochondrial biogenesis is a common feature to myocardial hypertrophy and end-stage ischemic heart failure. *Cardiovasc Pathol*. 25(2):103-112.
139. Lebrecht D, Setzer B, Ketelsen UP, Haberstroh J, Walker UA. (2003) Time-dependent and tissue-specific accumulation of mtDNA and respiratory chain defects in chronic doxorubicin cardiomyopathy. *Circulation*. 108(19):2423-2429.
140. Tsutsui H, Ide T, Kinugawa S. (2006) Mitochondrial oxidative stress, DNA damage and heart failure. *Antioxid Redox Signal*. 9-10:1737-1744.
141. Torres S, Divi RL, Walker DM, McCash CL, Carter MM, et al. (2010) In utero exposure of female CD-1 mice ot AZT and/or 3TC: II. Persistence of functional alterations in cardiac tissue. *Cardiovasc Toxicol*. 10(2):87-99.
142. Oka T, Hikoso S, Yamaguchi O, Taneike M, Takeda T, et al. (2012) Mitochondrial DNA that escapes from autophagy causes inflammation and heart failure. *Nature*. 485(7397):251-255.
143. Suliman H, Carraway MS, Tatro LG, Piantadosi CA. (2006) A new activating role for CO in cardiac mitochondrial biogenesis. *J Cell Sci*. 120(2):299-308.
144. Kluza J, Marchetti P, Gallego MA, Lancel S, Fournier C, et al. (2004) Mitochondrial proliferation during apoptosis induced by anticancer agents: effects of doxorubicin and mitoxantrone on cancer and cardiac cells. *Oncogene*. 23(42):7018-7030.
145. Alvarez-Garcia O, Matsuzaki T, Olmer M, Plate L, Kelly JW, et al. (2017) Regulated in development and DNA damage response 1 deficiency impairs autophagy and mtiochondrial biogenesis in articular cartilage and increases the severity of experimental osteoarthritis. *Arthritis Theumatol*. 69(7):1418-1428.
146. Fu X, Wan S, Lyu YL, Liu LF, Qi H. (2008) Etoposide induces ATM-dependent mitochondrial biogenesis through AMPK activation. *PLoS One*. 3(4):e2009.

147. Yoboue E, Mougeolle A, Kaiser L, Averet N, Rigoulet M, et al. (2014) The role of mitochondrial biogenesis and ROS in the control of energy supply in proliferating cells. *Biochim Biophys Acta*. 1837(7):1093-1098.
148. Bellavia A, Urch B, Speck M, Brook RD, Scott JA, et al. (2013) DNA hypomethylation, ambient particulate matter, and increased blood pressure: findings from controlled human exposure experiments. *J Am Heart Assoc*. 2(3):e000212.
149. Soberanes S, Gonzalez A, Urich D, Chiarella SE, Radigan KA, et al. (2012) Particulate matter air pollution induces hypermethylation of the p16 promoter via a mitochondrial ROS-JNK-DNMT1 pathway. *Sci Rep*. 2:275.
150. Jardim M, Fry RC, Jaspers I, Dailey L, Diaz-Sanchez D. (2009) Disruption of microRNA expression in human airway cells by diesel exhaust particles is linked to tumorigenesis-associated pathways. *Environmental Health Perspectives*. 117(11):1745-51.
151. Liu J, Ballaney M, Al-alem U, Quan C, Jin X, Perera F, Chen L, Miller RL. (2008) Combined inhaled diesel exhaust particles and allergen exposure alter methylation of T helper genes and IgE production *in vivo. Toxicological Sciences*. 102(1):76-81.
152. Khalil C. (2014) The emerging role of epigenetics in cardiovascular disease. *Therapeutic Advances in Chronic Disease*. 5(4):178-187.
153. Zhong J, Agha G, Baccarelli AA. (2016) The role of DNA methylation in cardiovascular risk and disease. *Circ Res*. 118:119-131.
154. Bird A. (2002) DNA methylation patterns and epigenetic memory. *Genes Dev*. 16(1):6-21.
155. Plusquin M, Guida F, Polidoro S, Vermeulen R, Raaschou-Nielsen O, et al. (2017) DNA methylation and exposure to ambient air pollution in two prospective cohorts. *Environ Int*. 108:127-136.
156. Turk P, Laayoun A, Smith SS, Weitzman SA. (1995) DNA adduct 8-hydroxyl-2'-deoxyguanosine (8-hydroxyguanine) affects function of human DNA methyltransferase. *Carcinogenesis*. 16(5):1253-1255.
157. Glier M, Green TJ, Devlin AM. (2013) Methyl nutrients, DNA methylation, and cardiovascular disease. *Mol Nutr Food Res*. 58(1):172-182.
158. Berk M, Malhi GS, Gray LJ, Dean OM. (2013) The promise of N-acetylcysteine in neuropsychiatry. *Trends Pharmacol Sci*. 34(3):167-177.
159. Palinkski W, Napoli C. (2002) The fetal origins of atherosclerosis: maternal hypercholesterolemia, and cholesterol-lowering or antioxidant treatment during pregnancy influence in utero programming and postnatal susceptibility to atherogenesis. *FASEB J*. 16(11):1348-1360.
160. Lee B, Hong YC, Lee KH, Kim YJ, Kim WK, et al. (2004) Influence of maternal serum levels of vitamins C and E during the second trimester on birth weight and length. *Eur J Clin Nutr*. 58(10):1365-1371.
161. Baccarelli A, Cassano PA, Litonjua A, Park SK, Suh H, et al. (2008) Cardiac autonomic dysfunction: effects from particulate air pollution and protection by dietary methyl nutrients and metabolic polymorphisms. *Circulation*. 117(14):1802-1809.

162. Lertratanangkoona K, Wub CJ, Savarajb N, Thomasa ML. (1997) Alterations of DNA methylation by glutathione depletion. *Cancer Lett*. 120(2):149-56.
163. García-Giménez J, Pallardó FV. (2014) Maintenance of glutathione levels and its importance in epigenetic regulation. *Front Pharmacol*. 5:88.
164. Grollman A, Moriya M. (1993) Mutagenesis by 8-oxoguanine: an enemy within. *Trends Genet*. 9(7):246-249.

Jamie Michelle Goodson
307 NE 43rd St
Seattle, WA 98105
(253) 970-7709
goodsj@u.washington.edu

Education

University of Washington, Seattle WA
Bachelor of Science, Graduated June 2011
Major: Molecular, Cellular and Developmental Biology

University of Washington, Seattle WA
Department of Pathology
September 2013-Present

Publications

Goodson JM, Weldy CS, MacDonald JW, Liu Y, Bammler TK, Chien W, Chin MT. *In utero* exposure to diesel exhaust particulates is associated with an altered cardiac transcriptional response to transverse aortic constriction and altered DNA methylation. *FASEB Journal*. 2017;31(11):4935-4945. doi: 10.1096/fj.201700032R.

Choi M, Genereux DP, **Goodson J**, Al-Assawi H, Allain SQ, Simon N, Palasek S, Ware CB, Cavanaugh C, Miller DG, Johnson WC, Sinclair KD, Stöger R, Laird CD. Epigenetic memory *via* concordant DNA methylation is inversely correlated to developmental potential of mammalian cells. *PLoS Genetics*. 2017;13(11):e1007060. doi: 10.1371/journal.pgen.1007060.

Liu Y, **Goodson JM**, Zhang B, Chin MT. Air pollution and adverse cardiac remodeling: clinical effects and basic mechanisms. *Frontiers in Physiology*. 2015;6:162. doi:10.3389/fphys.2015.00162.

Yang PT, Anastas JN, Toroni RA, Shinohara MM, **Goodson JM**, Bosserhoff AK, Chien AJ, Moon RT. WLS inhibits melanoma cell proliferation through the beta-catenin signaling pathway and induces spontaneous metastasis. *EMBO Molecular Medicine*. 2012;4(12):1294-1307. doi:10.1002/emmm.201201486.

Davidson, K.C., Adams, A.M., **Goodson, J.M.**, McDonald, C.E., Potter, J.C, Biechele, T.L., Taylor, R.J, Moon, R.T. Wnt/β-catenin signaling promotes differentiation, not self-renewal, of human embryonic stem cells and is repressed by Oct4. *Proceedings of the National Academy of Sciences of the United States of America*. 2012;109(12):4485-4490. doi:10.1073/pnas.1118777109.

White, B.D., Nathe, R.J., Maris, D.O., Nguyen, N.K., **Goodson, J.M.**, Moon, R.T., Horner, P.J., β-Catenin Signaling Increases in Proliferating NG2+ Progenitors and Astrocytes during Post-Traumatic Gliogenesis in the Adult Brain. *Stem cells*. 2010;28(2):297-307. doi:10.1002/stem.268.

Awards

Environmental Pathology and Toxicology Training Grant: August 2014-2017
Communications Fellowship Award (Seattle Pacific Science Center): February 2016
HHMI/UW Molecular Medicine Scholar Award: April-May 2015
Association of Women in Science Scholarship: Fall quarter 2010
Mary Gates Scholarship: Winter and Spring quarters 2010

Teaching Experience

Teacher's Assistant for Biology 180: Spring Quarter 2011
University of Washington

Volunteer Experience

Pacific Science Center Volunteer: February 2016-Present
South Lake Union Group (SLUG) Committee Member: September 2014- June 2016
Seattle Expanding Your Horizons Committee Member: September 2012-March 2016